A Primer on CP Violation in the B^0-$\bar{B}^0$ System

Kirk T. McDonald
Joseph Henry Laboratories, Princeton University, Princeton, NJ 08544
(May 25, 1990; updated August 15, 2013)

After the discovery of parity violation in weak interactions in 1957 [1], Landau [2], as well as Lee and Yang [3], proposed that this interaction is invariant with respect to the combined operations of charge conjugation and spatial inversion, since called CP invariance. In 1964, Christenson, Cronin, Fitch and Turlay reported observation of decay of the K_L^0 meson, then thought to be the CP-odd state $(|K^0\rangle - |\bar{K}^0\rangle)/\sqrt{2}$ into the CP-even final state $\pi^+\pi^-$ [4].[1] The so-called superweak theory was postulated shortly thereafter [6, 7, 8], that CP violation would be confined to the K^0-$\bar{K}^0$ system, and indeed until the observation of CP violation in the B^0-$\bar{B}^0$ system in 2001 [9, 10] this remained the case.

Manifestations of CP violation are richer in the B-meson system than in mesons with only the lighter quarks u, d, s and c, for which only the K^0-$\bar{K}^0$ system exhibits this phenomenon.

1 CP Violation in the K-Meson System

The usual path to understanding CP violation in the B-meson system begins by comparison with the K-meson system. In the latter, the states $|K^0\rangle$ and $|\bar{K}^0\rangle$ are eigenstates of the strong and electromagnetic interactions, which conserve strangeness. However, these states are not eigenstates of the weak interactions, which violate strangeness, and which are responsible for Kaon decay. For example, a $K^0 = d\bar{s}$ can transform into a $\bar{K}^0 = \bar{d}s$ via the weak interaction described by the box diagram in Fig. 1 (from [11]).[2]

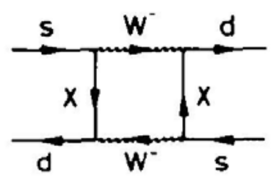

Figure 1: Box diagram for the transition $|K^0\rangle \leftrightarrow |\bar{K}^0\rangle$, where X is a u, c or t quark.

Taking into account the weak interactions, one writes the 2×2 Hamiltonian (in the $|K^0\rangle$-$|\bar{K}^0\rangle$ basis) as,

$$\mathsf{H} = \mathsf{M} - \frac{i}{2}\Gamma, \tag{1}$$

where the mass matrix M and the decay matrix Γ are Hermitian.[3] (Since neutral Kaons decay, H itself is not Hermitian.) CPT invariance implies that the diagonal components of

[1] Cronin traces the history of this discovery in [5].

[2] The Feynman rules for computations of such diagrams indicate that the dominant contribution is from the quark with mass closest to that of the W boson, namely the top quark [12].

[3] The classic reference on this topic is the 1966 review by Lee and Wu [13].

H are equal, and if CP is conserved M and Γ are real. Allowing for the possibility of CP violation, the Hamiltonian can be written as,

$$\mathsf{H} = \begin{bmatrix} m & M_{12} \\ M_{12}^* & m \end{bmatrix} - \frac{i}{2}\begin{bmatrix} \gamma & \Gamma_{12} \\ \Gamma_{12}^* & \gamma \end{bmatrix}. \tag{2}$$

Solving $|\mathsf{H} - \lambda \mathsf{I}| = \lambda^2 - 2H_{11}\lambda + H_{11}^2 - H_{12}H_{21} = 0$ for the eigenvalues λ, we find,

$$\lambda = H_{11} \pm \sqrt{H_{12}H_{21}} = m \pm \mathrm{Re}\sqrt{H_{12}H_{21}} - \frac{i}{2}\left(\gamma \mp 2\,\mathrm{Im}\sqrt{H_{12}H_{21}}\right) \tag{3}$$

where the state with the longer lifetime (smaller Γ), $|K_L^0\rangle$, has higher mass than the shorter-lived state $|K_S^0\rangle$,

$$m_{L,S} = m \pm \frac{\Delta m}{2} = m \pm \mathrm{Re}\sqrt{H_{12}H_{21}}\,, \qquad \Gamma_{L,S} = \gamma \mp \frac{\Delta\Gamma}{2} = \gamma \mp 2\,\mathrm{Im}\sqrt{H_{12}H_{21}}. \tag{4}$$

The mass and width differences between the states $|K_L^0\rangle$ and $|K_S^0\rangle$ are given by,[4]

$$\begin{aligned} \Delta m &= 2\,\mathrm{Re}\left[\left(M_{12} - \tfrac{i}{2}\Gamma_{12}\right)\left(M_{12}^* - \tfrac{i}{2}\Gamma_{12}^*\right)\right]^{1/2}, \\ \Delta\Gamma &= 4\,\mathrm{Im}\left[\left(M_{12} - \tfrac{i}{2}\Gamma_{12}\right)\left(M_{12}^* - \tfrac{i}{2}\Gamma_{12}^*\right)\right]^{1/2}. \end{aligned} \tag{5}$$

We define the eigenstates via the complex coefficients p and q, where $|p|^2 + |q|^2 = 1$, according to,

$$|K_{L,S}^0\rangle = p|K^0\rangle \mp q|\bar{K}^0\rangle, \qquad |K^0\rangle = \frac{|K_S^0\rangle + |K_L^0\rangle}{2p}, \qquad |\bar{K}^0\rangle = \frac{|K_S^0\rangle - |K_L^0\rangle}{2q}. \tag{6}$$

Then, $\mathsf{H}|K_S^0\rangle = \lambda_S|K_S^0\rangle$, and, say, the $|K^0\rangle$ component of this relation implies that,

$$\frac{q}{p} \equiv \frac{1-\epsilon}{1+\epsilon} = \sqrt{\frac{H_{21}}{H_{12}}} = \sqrt{\frac{M_{12}^* - \frac{i}{2}\Gamma_{12}^*}{M_{12} - \frac{i}{2}\Gamma_{12}}} = \frac{H_{21}}{\sqrt{H_{12}H_{21}}} = 2\frac{M_{12}^* - \frac{i}{2}\Gamma_{12}^*}{\Delta m - \frac{i}{2}\Delta\Gamma}. \tag{7}$$

In terms of the parameter ϵ, the states are,

$$|K_S^0\rangle = \frac{(1+\epsilon)|K^0\rangle + (1-\epsilon)|\bar{K}^0\rangle}{\sqrt{2(1+|\epsilon|^2)}}, \qquad |K^0\rangle = \frac{\sqrt{2(1+|\epsilon|^2)}}{2(1+\epsilon)}\left[|K_S^0\rangle + |K_L^0\rangle\right], \tag{8}$$

$$|K_L^0\rangle = \frac{(1+\epsilon)|K^0\rangle - (1-\epsilon)|\bar{K}^0\rangle}{\sqrt{2(1+|\epsilon|^2)}}, \qquad |\bar{K}^0\rangle = \frac{\sqrt{2(1+|\epsilon|^2)}}{2(1-\epsilon)}\left[|K_S^0\rangle - |K_L^0\rangle\right]. \tag{9}$$

If M and Γ were real, then $p = q$ and ϵ would be zero, so that a nonzero ϵ is evidence for $\Delta S = 2$ CP violation.[5] (In the limit of vanishing ϵ, the weak states would be CP eigenstates:

[4] The mass difference $|\Delta m|$ was first measured in [14, 15], and the sign was first determined in [16, 17, 18]. $\Delta m/m \approx 7\times 10^{-15}$, and $\Delta m/\Gamma \approx 2\Delta m/\Gamma_S \approx 0.94$.

[5] A nonzero value for ϵ was first measured by [4]. The present best value is $|\epsilon| = 0.00223 \pm 0.00001$.

$K_S^0 \to K_1^0$ would have CP +; $K_L^0 \to K_2^0$ would have CP −.) This will be referred to as CP violation in the mixing, which is observable because of the substantial difference in the lifetimes of the K_S^0 (9×10^{-11} s) and the K_L^0 (5×10^{-8} s).

It is also possible to have (direct) CP violation in the decays of Kaons, parameterized by the $\Delta S = 1$ CP-violating parameter ϵ', which arises from different isospin phases in the amplitudes for the decays $K \to 2\pi$,

$$\begin{aligned} a_0 &= \langle \pi\pi,\ I = 0\,|H_W|K^0\rangle \ , \\ a_2 &= \langle \pi\pi,\ I = 2\,|H_W|K^0\rangle \ , \end{aligned} \tag{10}$$

and,

$$\epsilon' \propto \mathrm{Im}\left(\frac{a_2}{a_0}\right) \ . \tag{11}$$

In the Standard Model, it is expected that $\epsilon' \ll \epsilon$, and experimentally one finds [19, 20] that,

$$\frac{\epsilon'}{\epsilon} \approx 10^{-3}. \tag{12}$$

Therefore, in the Kaon system, CP violation with $\Delta S = 2$ is much larger than that with $\Delta S = 1$.

2 CP Violation in the B-Meson System

The neutral B-mesons $B_d^0 = d\bar{b}$ and $B_s^0 = s\bar{b}$ have relatively long lifetimes, $\tau_{B_d^0} = 1.52 \times 10^{-12}$ s (first measured in [21, 22]), $\tau_{B_s^0} = 1.51 \times 10^{-12}$ s (first measured in [23]),[6] such that the decay point of a B^0-meson can be resolved from its production point, permitting studies of B^0-$\bar{B}^0$ mixing as a function of time.

2.1 Mixing Analysis

For B-mesons, the mixing formalism is identical to that given in eqs. (1)-(9). However, there are some significant differences between the B-meson and the K-meson systems. First of all, since B mesons are so heavy, the phase space for their decays is quite large. Therefore, both B and $\bar{B}$ have essentially the same lifetime, so that $\Delta\Gamma/\Gamma \ll 1$. We will not label the eigenstates of the B-meson system with subscripts S and L, but with subscripts + and -, where $|B_+^0\rangle$ has higher mass than $|B_-^0\rangle$.

Furthermore, calculations [24] based on the box diagram in the Standard Model have shown that, for the B-meson system, $\Gamma_{12} \ll M_{12}$, which leads to the result that $\Delta\Gamma \ll \Delta M$. (We note that this is quite different than the K-meson system, where there is a substantial lifetime difference, due to the differing phase space for the 2π and 3π channels.) We will therefore neglect $\Delta\Gamma$ in what follows for the B-meson system.

[6]For comparison, $\tau_{D^0} = 4.1 \times 10^{-13}$ s.

For the same reason, the $\Delta B = 2$ CP-violating parameter in the B system, ϵ_B, is also small,

$$\left|\frac{1-\epsilon_B}{1+\epsilon_B}\right| = \left|\frac{q}{p}\right| \simeq 1 - \frac{1}{2}\,\mathrm{Im}\,\frac{\Gamma_{12}}{M_{12}} \approx 1, \tag{13}$$

So the ratio p/q is essentially a pure phase for B-mesons.

The CP eigenstates of the neutral B-meson system can now be written as,

$$\begin{aligned} |B^0_+\rangle &= p|B^0\rangle + q|\bar{B}^0\rangle, \qquad & |B^0\rangle &= \tfrac{|B^0_+\rangle + |B^0_-\rangle}{2p}\,, \\ |B^0_-\rangle &= p|B^0\rangle - q|\bar{B}^0\rangle, \qquad & |\bar{B}^0\rangle &= \tfrac{|B^0_+\rangle - |B^0_-\rangle}{2q}\,. \end{aligned} \tag{14}$$

Because the lifetimes of the B^0_+ and B^0_- are nearly the same ($\Delta\Gamma_d/\Gamma_d \approx 1/60$, $\Delta\Gamma_s/\Gamma_s \approx 1/6$), distinguishing these states to exhibit CP violating in the mixing is not practical.[7]

However, in the B-system, one situation is reversed with respect to the Kaon system, namely, "direct" CP violation in B-decays ($\Delta B = 1$) can be large. To have an observable effect of CP violation, there must be interference between two decay amplitudes with different phases, as discussed further in sec. 2.3.1.

A relevant parameter for B-$\bar{B}$ mixing is x_q, the ratio of the energy of the oscillation (*i.e.*, the mass difference) and the total width for the B_q mesons ($q = d, s$),

$$x_q = \frac{\Delta M_q}{\Gamma_q} = \frac{(\text{transition energy})}{(\text{mean total width})}\ . \tag{15}$$

After all, mixing hardly matters if the particle decays before it has a chance to oscillate into its antiparticle. The mixing parameter for B^0_d-mesons is $x_d = 0.78$ (first measured in [26, 27]), while that for B^0_s-mesons is $x_s = 26$ (first measured in [28, 29]).[8] The large value of x_s permits multiple meson-antimeson oscillations to be observed more easily in the B^0_s-system than in any other, as shown in Fig. 2.

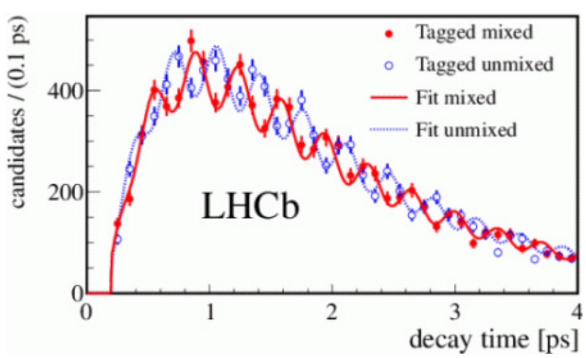

Figure 2: B^0_s-$\bar{B}^0_s$ oscillations as observed in [32].

The role of the mixing parameter x can be seen explicitly by considering the time evolution of B mesons. Because of B^0-$\bar{B}^0$ mixing, a state which starts out as a pure B^0 or $\bar{B}^0$

[7]This may have been first discussed in [25].

[8]For comparison, the mixing parameter for D^0-mesons is $x = 0.6$ (first measured in [30, 31]), while for K^0-mesons $x = 0.94$ as noted earlier.

will evolve in time to a mixture of B^0 and $\bar{B}^0$,

$$
\begin{aligned}
|B^0\rangle &= \frac{|B^0_+\rangle + |B^0_-\rangle}{2p} \to \frac{1}{2p}\left[e^{-iM_+t}e^{-\Gamma t/2}|B^0_+\rangle + e^{-iM_-t}e^{-\Gamma t/2}|B^0_-\rangle\right], \\
&= \frac{e^{-\Gamma t/2}}{2p}\left\{e^{-i(M+\Delta M/2)t}\left[p|B^0\rangle + q|\bar{B}^0\rangle\right] + e^{-i(M-\Delta M/2)t}\left[p|B^0\rangle - q|\bar{B}^0\rangle\right]\right\}, \\
&= F_+(t)|B^0\rangle + \frac{q}{p}F_-(t)|\bar{B}^0\rangle\ , \qquad (16) \\
|\bar{B}^0\rangle &\to \frac{p}{q}F_-(t)|B^0\rangle\ + F_+(t)|\bar{B}^0\rangle\ , \qquad (17)
\end{aligned}
$$

where,

$$
\begin{aligned}
F_+(t) = &\quad e^{-iMt}e^{-\Gamma t/2}\cos(\Delta M t/2) = e^{-iM\tilde{t}/\Gamma}e^{-\tilde{t}/2}\cos(x\tilde{t}/2), \\
F_-(t) = &\ ie^{-iMt}e^{-\Gamma t/2}\sin(\Delta M t/2) = ie^{-iM\tilde{t}/\Gamma}e^{-\tilde{t}/2}\sin(x\tilde{t}/2),
\end{aligned}
\qquad (18)
$$

$\tilde{t} = t/\Gamma$ measures time in units of the B-lifetime Γ, and $x = \Delta\Gamma/M$ is the mixing parameter defined in eq. (15).

2.2 The CKM Quark-Mixing Matrix

Before discussing CP violation in B-meson decay it is useful to introduce the so-called CKM quark-mixing matrix (named after Cabibbo [33], Kobayashi and Maskawa [34]).

The issue is that the weak interactions of the quarks u, c, t, d, s and b as participate in the strong interaction do not have simple weak-interaction couplings $u \leftrightarrow W^+d$, $c \leftrightarrow W^+s$, $t \leftrightarrow W^+b$, but rather these weak couplings can be represented as $u \leftrightarrow W^+d'$, $c \leftrightarrow W^+s'$, $t \leftrightarrow W^+b'$, via the notation,

$$
\begin{pmatrix} d' \\ s' \\ b' \end{pmatrix} = V_{\rm CKM}\begin{pmatrix} d \\ s \\ b \end{pmatrix} \equiv \begin{pmatrix} V_{ud} & V_{us} & V_{ub} \\ V_{cd} & V_{cs} & V_{cb} \\ V_{td} & V_{ts} & V_{tb} \end{pmatrix}\begin{pmatrix} d \\ s \\ b \end{pmatrix}, \qquad (19)
$$

where $V_{\rm CKM}$ is a unitary matrix, and V_{us} is the (relative) strength of the coupling $u \leftrightarrow W^+s$, *etc.* The matrix elements can (unfortunately) be written many ways, with an early form given in [35], while the now-standard form (introduced in [36]) writes c_{13} for $\cos\theta_{12}$, s_{23} for $\sin\theta_{23}$, *etc.*, where θ_{12}, θ_{13} and θ_{23} are mixing angles,

$$
\begin{aligned}
V_{\rm CKM} &= \begin{pmatrix} c_{12} & s_{12} & 0 \\ -s_{12} & c_{12} & 0 \\ 0 & 0 & 1 \end{pmatrix}\begin{pmatrix} 1 & 0 & 0 \\ 0 & c_{23} & s_{23} \\ 0 & -s_{23} & c_{23} \end{pmatrix}\begin{pmatrix} c_{13} & 0 & s_{13}\,e^{-i\delta} \\ 0 & 1 & 0 \\ -s_{13}\,e^{i\delta} & 0 & c_{13} \end{pmatrix} \\
&= \begin{pmatrix} c_{12}c_{13} & s_{12}c_{13} & s_{13}\,e^{-i\delta} \\ -s_{12}c_{23} - c_{12}s_{23}s_{13}\,e^{-i\delta} & c_{12}c_{23} - s_{12}s_{23}s_{13}\,e^{-i\delta} & s_{23}c_{13} \\ s_{12}s_{23} - c_{12}c_{23}s_{13}\,e^{-i\delta} & -c_{12}s_{23} - s_{12}c_{23}s_{13}\,e^{-i\delta} & c_{23}c_{13} \end{pmatrix}. \qquad (20)
\end{aligned}
$$

This form is also standard in the description of three-neutrino mixing, where it is called the Maki-Nakagawa-Sakata matrix [37] (where the mixing angles θ_{ij} and the CP-violating phase δ have different values and a different physical context; CP violation is expected in neutrino mixing). The notion of neutrino mixing preceded that of quark mixing, but experimental evidence for the latter came first.

A popular approximation to the CKM-matrix is due to Wolfenstein [38],

$$\begin{pmatrix} V_{ud} & V_{us} & V_{ub} \\ V_{cd} & V_{cs} & V_{cb} \\ V_{td} & V_{ts} & V_{tb} \end{pmatrix} \approx \begin{pmatrix} 1-\frac{\lambda^2}{2}+\frac{\lambda^4}{24} & \lambda & A\lambda^3(\bar\rho - i\bar\eta) \\ -\lambda & 1-\frac{\lambda^2}{2}-\lambda^4(\frac{A^2}{8}-\frac{1}{24}) & A\lambda^2 \\ A\lambda^3(1-\bar\rho-i\bar\eta) & -A\lambda^2+A\lambda^4(\frac{1}{2}-\rho-i\eta) & 1-\frac{A^2\lambda^4}{2} \end{pmatrix}, \tag{21}$$

in which the expansion parameter λ is essentially the sine of the Cabibbo angle.[9] A variant is to define $\rho\, e^{i\delta} = \bar\rho + i\bar\eta$ such that $V_{ub} = A\lambda^3 \rho\, e^{-i\delta}$ and $V_{td} = A\lambda^3(1-\rho\, e^{i\delta})$.

The existence of CP violation in the quark sector corresponds to nonzero $\bar\eta$ and δ, which appear most prominently in matrix elements V_{ub} and V_{td}. The latter plays a role in the box diagram, Fig. 1, and hence in meson-antimeson mixing (including K^0-$\bar K^0$ mixing), but they do not appear at first order in decay amplitudes of mesons containing only u, d, s and c quarks. Hence "direct" CP violation will only be significant in the B-meson system.[10]

The present state of fits to the Wolfenstein parameters is displayed at, for example, http://ckmfitter.in2p3.fr/

The present fit values are $A = 0.82$, $\lambda = 0.22$, $\bar\rho = 0.13$, $\bar\eta = 0.35$, $\rho = 0.37$, $\delta = 70^\circ$.[11]

An example of the use of the CKM-matrix is in a comparison of the mixing parameters x_d and x_s of eq. (15), for B_d^0 and B_s^0-mesons, respectively. The meson-antimeson oscillations are associated with the box diagram of Fig. 1, which is dominated by exchange of the top quark (as mentioned in footnote 2). Hence, to a first approximation,

$$\frac{x_s}{x_d} \approx \frac{|V_{ts}|^2}{|V_{td}|^2} \approx \frac{1}{\lambda^2\,|1-\bar\rho-i\bar\eta|^2} - \frac{1}{\lambda^2[(1-\bar\rho)^2+\bar\eta^2]} \approx 23.5, \tag{22}$$

which compares reasonably well to the experimental value of 33 for this ratio.

2.2.1 The Unitarity Triangle

The CKM matrix is unitary, and describes the behavior of the weak interaction of quarks under a change of basis of the quark states. Consideration of aspects of CP violation are independent of the choice of basis led Jarlskog [40] to note the existence of an invariant property of certain combinations of CKM-matrix elements. Namely, if,

$$\begin{pmatrix} V_{ij} & V_{ik} \\ V_{lj} & V_{lk} \end{pmatrix} \tag{23}$$

[9] The expansion to fourth order in λ is from [39], which slightly modified the form given in [38] to become a better approximation to the now-standard form (20).

[10] Mesons containing t quarks decay quickly to ones containing b quarks, with amplitude $\propto V_{tb}$ which does not involve CP violation.

[11] in 1990 the values of $\bar\rho$ and $\bar\eta$ were very poorly known, as represented by the band labeled ϵ_K is Fig. 4.

is the 2×2 submatrix obtained by deleting row m and column n of V_{CKM}, then,

$$J = (-1)^{m+n}\,\mathrm{Im}[V_{ij} V_{lk} V^\star_{ik} V^\star_{lj}] \tag{24}$$

is the same for any choice of $m\ n$. Comparison with the forms (21)-(20) show that the Jarlskog invariant J is nonzero only if $\bar\eta$ and δ are nonzero, *i.e.*, only if CP violation exists.[12]

A useful geometric interpretation of the Jarlskog invariant was given by Bjorken [41, 42] (see also [43]),[13] noting that the unitarity of the CKM-matrix implies that the products of column "vectors" of V_{CKM} with row "vectors" of $V^\dagger_{CKM}$ obey,

$$\sum_i V_{ij} V^\star_{ik} = \delta_{jk}, \qquad \sum_j V_{ij} V^\star_{kj} = \delta_{ik}. \tag{25}$$

In particular,

$$V_{ud} V^\star_{ub} + V_{cd} V^\star_{cb} + V_{td} V^\star_{tb} = 0, \qquad \frac{V_{ud} V^\star_{ub}}{V_{cd} V^\star_{cb}} + 1 + \frac{V_{td} V^\star_{tb}}{V_{cd} V^\star_{cb}} = 0, \tag{26}$$

so the three complex numbers, 1, $V_{td} V^\star_{tb}/V_{cd} V^\star_{cb}$ and $V_{ud} V^\star_{ub}/V_{cd} V^\star_{cb}$, if considered as "vectors" and placed "head to tail," form a triangle on the complex plane.

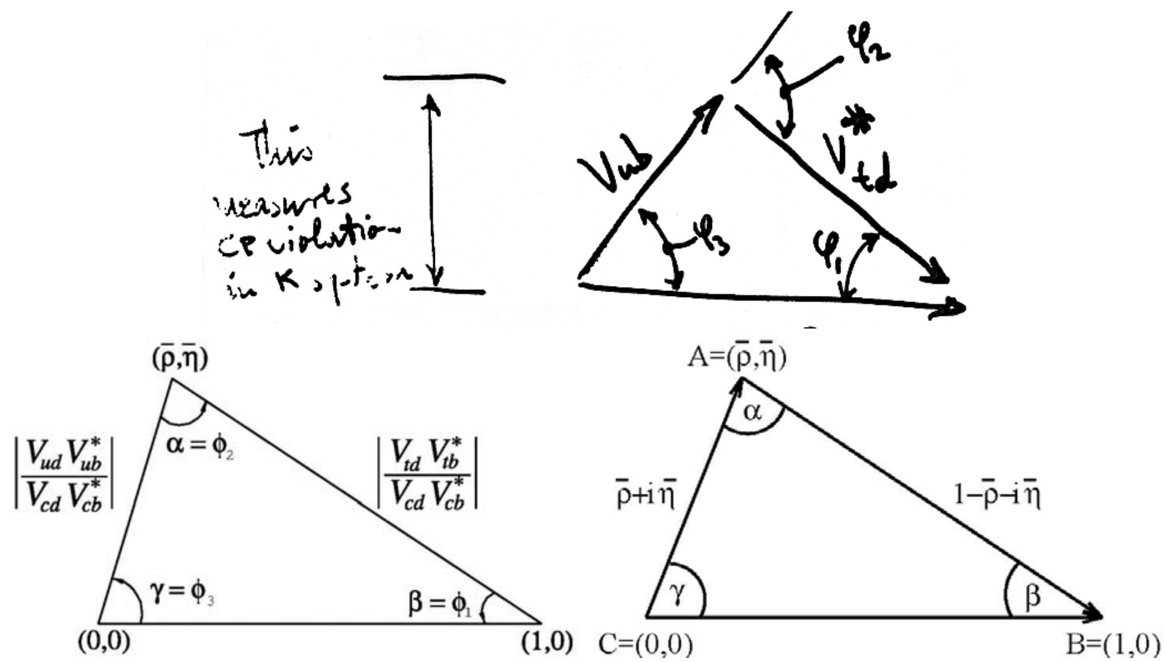

Figure 3: Versions of the unitarity triangle, with the upper version from [41].

Noting the directions of the "vector" sides of the triangle its, area is[14]

$$A = -\frac{1}{2}\,\mathrm{Im}\left[\frac{V_{ud} V^\star_{ub}}{V_{cd} V^\star_{cb}}\right] = \frac{-\,\mathrm{Im}[V_{ud} V_{cb} V^\star_{ub} V^\star_{cd}]}{2\,|V_{cd}|^2\,|V_{cb}|^2} = \frac{J}{2\,|V_{cd}|^2\,|V_{cb}|^2} \approx \frac{\bar\eta}{2}\left(1 - \frac{\lambda^2}{2}\right). \tag{27}$$

[12] In the parameterization of eq. (20), $J = c_{12} c_{23} c^2_{13} s_{12} s_{23} s_{13} \sin\delta$.

[13] Use of triangles to illustrate relations among complex CP-violating amplitudes was made earlier in [36, 44].

[14] The area of the triangle whose sides are the "vectors" $V_{ud} V^\star_{ub}$, $V_{cd} V^\star_{cb}$ and $V_{td} V^\star_{tb}$ is simply $J/2$.

That is, the Jarlskog invariant is proportional to the area of the so-called unitarity triangle, and this area is approximately the one half of CP-violating parameter $\bar{\eta} = \rho \sin \delta$.

The interior angles of the unitarity triangle are (unfortunately) called by two different conventions,[15]

$$\begin{aligned}
\phi_1 = \beta \quad &= 2\pi - \phi(V_{td}) &&\equiv 2\pi - \phi_{td}, \\
\phi_2 = \alpha \quad &= \pi - \phi_1 - \phi_3 &&= -\pi + \phi_{td} + \phi_{ub}, \\
\phi_3 = \gamma \quad &= \phi(V_{ub}^*) = -\phi(V_{ub}) &&\equiv -\phi_{ub},
\end{aligned} \tag{28}$$

where ϕ_{ub} and ϕ_{td} are the phases of V_{ub} and V_{td}, respectively.[16] In principle, these angles (and the CP-violating phases) could be determined from measurements only of the magnitudes of the sides of the unitarity triangle, if indeed the complex quantities 1, $V_{td}V_{tb}^\star/V_{cd}V_{cb}^\star$ and $V_{ud}V_{ub}^\star/V_{cd}V_{cb}^\star$ actually form a closed triangle. Hence, one test of the CKM formalism is that the unitarity triangle is closed, and that the interior angles sum to π.

Results of measurements of parameters of the CKM-matrix are commonly displayed on a plot in the (complex) $(\bar{\rho}, \bar{\eta})$ plane, as in Fig. 4 from the `ckmfitter` site.

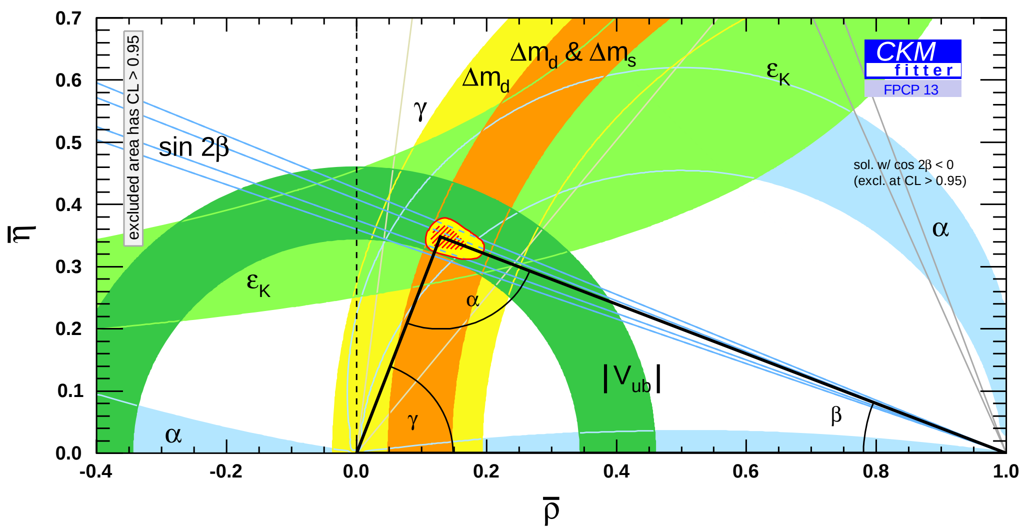

Figure 4: Present best fits to CKM-matrix parameters, displayed on the $(\bar{\rho}, \bar{\eta})$ plane. The band labeled ϵ_K is all that can be determined from the K^0-$\bar{K}^0$ system alone.

2.3 CP Violation in B-Meson Decay

We review six methods for measuring the CP-violating phases ϕ_{ub} and ϕ_{td} of the CKM-matrix via B-decays that are free from uncertainties due to strong final-state phases,

[15] The notation α, β, γ may have been introduced in [45].

[16] In the notation of eq. (20), $\phi_{ub} = \delta$. However, in the following we use the symbol δ to characterize a phase difference between two decay amplitudes, so we do not further use the symbol δ to mean the a CP-violating phase.

1. B decays to D^0X, $\bar{D}^0X$, and $D^0_{1,2}X$ where $X \neq \bar{X}$.

   Ex: $B^\pm \to D^0K^\pm$ [46] (the first observation of CP violation for charged mesons) and $B^0_d \to DK^{\star 0}$ measure ϕ_{ub} (*i.e.*, $\phi_3 = \gamma$).

2. Neutral B-meson decays to f and $\bar{f}$ where $f \neq \bar{f}$.

   Ex: $B^0_d \to D^\pm\pi^\mp$ measures $2\phi_{td} + \phi_{ub}$ and $B^0_s \to D^\pm_s K^\mp$ measures ϕ_{ub}.

3. Neutral B-meson decays to D^0X, $\bar{D}^0X$, and $D^0_{1,2}X$ where $X = \bar{X}$.

   Ex: $B^0_d \to DK^0_S$ measures ϕ_{ub}, $2\phi_{ub} + \phi_{td}$ and $\phi_{ub} + \phi_{td}$, and $B^0_s \to D\phi$ measures ϕ_{ub}.

4. Neutral B-meson decays to CP eigenstates.

   Ex: $B^0_d \to J/\psi K^0_S$ measures ϕ_{td} (*i.e.*, $\phi_2 = \beta$) [9, 10], $B^0_d \to \pi^+\pi^-$ measures $\phi_{td} + \phi_{ub}$, and $B^0_s \to \rho^0 K^0_S$ measures ϕ_{ub}.

5. B decays to sets of final states related by isospin.

   Ex: $B^0_d \to \pi^+\pi^-$, $\pi^0\pi^0$ and $B^+ \to \pi^+\pi^0$ measure $\phi_{td} + \phi_{ub}$ free from uncertainty due to penguin contributions.

6. Angular analysis of B decays to mixtures of CP eigenstates.

   Ex: $B^0_d \to J/\psi K^0_S\pi^0$ and $D^{\star+}D^{\star-}$ measure ϕ_{td}, and $B^0_d \to \rho^+\rho^-$ and $\rho^0\rho^0$ measure $\phi_{td} + \phi_{ub}$ (*i.e.*, $\phi_1 = \alpha$) [47, 48].

All of these except the well-known method 4 involve non-CP eigenstates. Methods 1-3 allow extraction of ϕ_{ub} from B_u and B_d, and will require greater emphasis on Kaon identification than methods 4-6. Methods 5 and 6 require photon detection in most cases. Method 1 does not require tagging of the particle/antiparticle character of the second B, and so could be used at a symmetric e^+e^- collider without the penalty due to mixing of methods 2-6. The mode $B^0_d \to J/\psi K^0_S$ which measures ϕ_{td} via method 4 is the most accessible of all those considered here.

2.3.1 The Need for Interference in CP-Violating Processes

In the Standard Model, CP violation in a process described by a single graph manifests itself only as a phase factor. If the amplitude for a single graph $B \to f$ is written,

$$A(B \to f) \equiv A_f = |A_f|\, e^{i\phi_W} e^{i\delta_S}, \tag{29}$$

where ϕ_W is a phase due to the weak interaction, and δ_S is a phase due to strong final-state interactions, then the CP conjugate process has amplitude,

$$A(\bar{B} \to \bar{f}) \equiv \bar{A}_{\bar{f}} = |A_f|\, e^{-i\phi_W} e^{i\delta_S}. \tag{30}$$

Hence CP violation cannot be discerned as a rate difference between a decay and its CP-conjugate decay if only a single graph contributes to the amplitude.

CP violation can only be revealed in *total-rate measurements* of $B \to f$ and $\bar{B} \to \bar{f}$ when there is interference between two or more decay amplitudes with differing weak phases *and* differing strong phases. To verify the last remark, consider the case where two graphs contribute to a decay, written as,

$$A(B \to f) = |A_1|\, e^{i\phi_1} e^{i\delta_1} + |A_2|\, e^{i\phi_2} e^{i\delta_2}, \tag{31}$$

so the CP-conjugate decay has amplitude,

$$A(\bar{B} \to \bar{f}) = |A_1|\, e^{-i\phi_1} e^{i\delta_1} + |A_2|\, e^{-i\phi_2} e^{i\delta_2}. \tag{32}$$

The corresponding decay rates are given by,

$$\Gamma(B \to f) = |A_1|^2 + |A_2|^2 + 2\,|A_1|\,|A_2| \cos(\phi + \delta), \tag{33}$$

and,

$$\Gamma(\bar{B} \to \bar{f}) = |A_1|^2 + |A_2|^2 + 2\,|A_1|\,|A_2| \cos(\phi - \delta), \tag{34}$$

where $\phi = \phi_1 - \phi_2$ and $\delta = \delta_1 - \delta_2$. Only if both ϕ and δ are nonvanishing can the interference term be determined from measurements of the two decay rates.

Even if this condition is satisfied the strong-interaction phase difference δ and the magnitudes $|A_f|$ and $\left|\bar{A}_{\bar{f}}\right|$ will not typically be known, and the CP-violating phase cannot be determined. In this note we examine six methods by which the uncertainties due to strong phases can be avoided. These are introduced in the following subsection, and then discussed in greater detail in the subsequent sections.

2.3.2 Six Methods for Extracting CP-Violating Phases

The most familiar method for study of the CP-violating phases in the CKM-matrix is called method 4 here. Method 1 is in some sense the most straightforward in principle, and can be used with charged B-mesons, and even with B-baryons. Methods 2-6 all utilize the mixing of neutral B-mesons to some extent, and hence are conceptually more complex.

A favorable theoretical result is that method 4, the study of neutral B decays to CP eigenstates, can in principle determine all three angles ϕ_i by measurement of three different decays [39]. However, the anticipated difficulty in measuring ϕ_{ub} via decays such as $B_s^0 \to \rho^0 K_S^0$, due to the small branching ratios (and poor signal of B_s at e^+e^- colliders), has been a motivation to explore the additional methods of analysis of CP violation reviewed in this paper.

1. **B decays to $D^0 X$, $\bar{D}^0 X$, and $D^0_{1,2} X$ where $X \neq \bar{X}$**

   When a B particle can decay both to $D^0 X$ and $\bar{D}^0 X$ (and so $\bar{B}$ decays to both $\bar{D}^0 \bar{X}$ and $D^0 \bar{X}$), then the decays

   $$B \to D^0_{1,2} X, \qquad \text{and} \qquad \bar{B} \to D^0_{1,2} \bar{X}, \qquad \text{where} \qquad D^0_{1,2} \equiv \frac{D^0 \pm \bar{D}^0}{\sqrt{2}}, \tag{35}$$

   exhibit a CP-violating asymmetry. Measurement of the six (or eight) decay modes listed will permit isolation of the CP-violating amplitude, both in magnitude and phase.

The final state D^0X need not be self conjugate, and it is actually desirable that it not be, so that no effects of mixing are present, and no tagging of the second B is needed. Thus, method 1 could be used at a symmetric e^+e^- collider without the penalty due to mixing of methods 2-6. This method works both for decays of B-mesons and b-baryons.

The general approach of methods 1-3 was largely anticipated by Carter and Sanda [49, 50], and more particularly by Gronau and London [51]. Method 1 as distinct from method 3 was first examined by Gronau and Wyler [52], with further discussions in [53, 54, 55]. Application of method 1 to b-baryons was first discussed by Aleksan, Dunietz and Kayser [56, 57].

If CP violation is found in such an analysis then it cannot be due to a superweak interaction [7, 8], which postulates that CP violation occurs only in mixing of neutral mesons. Thus, method 1 may be used to circumvent possible ambiguities [58] in the use of method 4 to prove or disprove the superweak model.

2. **Neutral B-meson decays to f and $\bar{f}$ where $f \neq \bar{f}$**

   If a neutral B-meson decays to both a final state f and its CP-conjugate state $\bar{f}$, then the interference of amplitudes needed for measurable CP violation arises due to mixing (whether or not there is CP violation in the mixing). A time-dependent analysis of the four decay modes $B(\bar{B}) \to f, \bar{f}$ can isolate the CP-violating phase.

   Tagging of the particle-antiparticle character of the second B in the event is required.

   The original paper on method 2 is by Gronau and London [51]. Discussion of method 2 as separate from method 3 was first been given by Aleksan *et al.* [59]. Method 2 is an improvement on earlier discussions by Du, Dunietz and Wu [60], and by Dunietz and Rosner [61], in which only two of the four related decays were utilized.

3. **Neutral B-meson decays to D^0X, $\bar{D}^0X$, and $D^0_{1,2}X$ where $X = \bar{X}$**

   If a neutral B-mesons decays to both a final state D^0X and $\bar{D}^0X$ where X is self conjugate ($CP(X) \equiv \bar{X} = \pm X$), then methods 1 and 2 can be combined. In a case of interest two different CP-violating phases can be determined from the time-dependent analysis of six (or eight) related decay modes.

   As previously mentioned, method 3 was first discussed by Gronau and London [51].

4. **Neutral B-meson decays to CP eigenstates**

   If a neutral B-meson decays to a final state f that is a CP eigenstate, then as in method 2, CP violation becomes observable via the interference due to mixing. But, since only a single final state is involved, the strong-interaction phase does not appear. Thus we recover the well-known result that a time dependent analysis of the two modes $B(\bar{B}) \to f$ can isolate the CP-violating phases.

   The advantages of measuring decays to CP eigenstates were first noted by Bigi and Sanda [62]. The important relation between decays to CP eigenstates and unitarity of the CKM matrix was first emphasized by Bjorken [41, 42], as discussed in sec. 2.2.1. The measurement of the three angles of the unitarity triangle by three specific decays to CP eigenstates was first proposed by Krawczyk *et al.* [39].

5. B **decays to sets of final states related by isospin**

   In decays $B_u^+ \to f^+$ and $B_d^0 \to f^0$ where the final states each arise due to the inference of two amplitudes, and f^+ and f^0 are related by isospin, the CP-violating phase can be isolated by a detailed isospin analysis.

   The utility of the isospin analysis in removing uncertainties due to penguin diagrams in B decays was first demonstrated by Gronau and London [63]. Further discussions have been given by Nir and Quinn [64], by Lipkin *et al.* [65] and by Gronau [66].

6. **Angular analysis of** B **decays to mixtures of** CP **eigenstates**

   If a neutral B-meson decays to a self-conjugate state f, but this is not a pure CP eigenstate (as holds when f consists of two spin-1 mesons) method 4 cannot be carried out. However, a detailed analysis of the angular distribution of the secondary-decay products can separate the final state into CP(even) and CP(odd) components and the CP-violating phase extracted.

   Methods of angular analysis for B decays to mixtures of CP eigenstates have been presented for several years [67, 68, 69], with more discussion by Kayser *et al.* [70], by Dunietz *et al.* [71], and by Kramer and Palmer [72, 73].

2.3.3 Time Dependence of a CP-Violating Asymmetry

Before discussing the six methods for measurement of CP violation in even greater detail, we note that these methods typically involve measurement of the time dependence of an asymmetry of the form,

$$A_f(t) = \frac{\Gamma(B^0(t) \to f) - \Gamma(\bar{B}^0(t) \to \bar{f})}{\Gamma(B^0(t) \to f) + \Gamma(\bar{B}^0(t) \to \bar{f})} \ . \tag{36}$$

If we consider a nonleptonic final state f such that both B^0 and $\bar{B}^0$ can decay both to it (and to its CP-conjugate state $\bar{f}$), this asymmetry can be calculated from eqs. (16)-(18). We have,

$$\begin{aligned} \Gamma(\overset{(-)}{B}{}^0(t) \to f) &= \left| \langle \overset{(-)}{f} | \overset{(-)}{B}{}^0(t) \rangle \right|^2 \\ &= \left| \langle \overset{(-)}{f} | \overset{(-)}{B}{}^0 \rangle \right|^2 e^{-t/\tau} \left[\cos^2 \tfrac{\Delta M t}{2} + \left| \overset{(-)}{\alpha}_f \right|^2 \sin^2 \tfrac{\Delta M t}{2} - \mathrm{Im}\, \overset{(-)}{\alpha}_f \sin \Delta M t \right] \end{aligned} \tag{37}$$

where we have introduced,

$$\alpha_f = \frac{q}{p}\, \rho_f \ , \qquad \bar{\alpha}_f = \frac{p}{q}\, \bar{\rho}_f \ , \tag{38}$$

and,

$$\rho_f = \frac{\langle f | \bar{B}^0 \rangle}{\langle f | B^0 \rangle} \ , \qquad \bar{\rho}_f = \frac{\langle \bar{f} | B^0 \rangle}{\langle \bar{f} | \bar{B}^0 \rangle} \ . \tag{39}$$

There are several points worth noting here. First of all, q/p is a pure phase, as noted in eq. (13). Secondly, **when only one amplitude contributes to** $B^0 \to f$ (and its CP-conjugate to $\bar{B}^0 \to \bar{f}$) then, recalling eqs. (29)-(30),

$$\left|\langle f|B^0\rangle\right| = \left|\langle \bar{f}|\bar{B}^0\rangle\right| , \qquad \left|\langle \bar{f}|B^0\rangle\right| = \left|\langle f|\bar{B}^0\rangle\right| , \tag{40}$$

i.e., $\left|\rho_f\right| = \left|\bar{\rho}_f\right|$. If there were no mixing there would now be no CP violation. However, in the presence of mixing the asymmetry (36) becomes,

$$A_f(t) = \frac{-(\mathrm{Im}\,\alpha - \mathrm{Im}\,\bar{\alpha})\sin\Delta Mt}{2\cos^2(\Delta Mt/2) + 2\left|\rho_f\right|^2 \sin^2(\Delta Mt/2) - (\mathrm{Im}\,\alpha + \mathrm{Im}\,\bar{\alpha})\sin\Delta Mt} \tag{41}$$

There may still be complications, however, due to ρ_f (and $\bar{\rho}_f$). To see this, recall the Wolfenstein approximation (21) to the CKM-matrix, in which large CP-violating phases appear only in V_{ub} and V_{td}. Then, one can estimate the size of certain B-decay diagrams just by counting powers of λ. For example, consider the final state $D^+\pi^-$. Here,

$$\begin{aligned} \langle D^+\pi^-|B^0\rangle &\sim V_{ub}^* V_{cd} \approx \mathcal{O}\left(\lambda^4\right) , \\ \langle D^+\pi^-|\bar{B}^0\rangle &\sim V_{cb} V_{ud}^* \approx \mathcal{O}\left(\lambda^2\right) . \end{aligned} \tag{42}$$

Therefore $\rho_f = \langle D^+\pi^- f|\bar{B}^0\rangle / \langle D^+\pi^-|B^0\rangle \approx \lambda^{-2} \approx 20$. According to eq. (36) the asymmetry goes like $1/\rho_f$ for large ρ_f, so it will be quite small for most values of t. If we had considered the final state $D^-\pi^+$, then we would have $\rho_f \sim \lambda^2 \sim 0.05$, and the asymmetry would again be small since $\mathrm{Im}\,\alpha_f$ is proportional to ρ_f. Furthermore, for both of these final states, hadronization effects are important. For example, for the final state $D^+\pi^-$ from B^0 decay the W hadronizes into the D, while from $\bar{B}^0$ decay it hadronizes into the π. There is no reliable way to calculate these effects.

These problems can be avoided by considering final states which are CP-eigenstates ($f = \pm\bar{f}$). Because of mixing, interference will occur between $\langle f|B^0\rangle$ and $\langle f|\bar{B}^0\rangle$, but now the latter is equal to $\pm\langle \bar{f}|\bar{B}^0\rangle$, which is equal in magnitude to $\langle f|B^0\rangle$ according to eq. (40). Hence, **the amplitude ratio ρ_f will also be a pure phase** (*i.e.*, $|\rho_f| = 1$).

For example, in the decay $B^0 \to \pi^+\pi^-$ we have,

$$\begin{aligned} \langle \pi^+\pi^-|B^0\rangle &\sim V_{ub}^* V_{ud} = A\rho\lambda^3 e^{i\delta}, \\ \langle \pi^+\pi^-|\bar{B}^0\rangle &\sim V_{ub} V_{ud}^* = A\rho\lambda^3 e^{-i\delta}. \end{aligned} \tag{43}$$

In addition, any hadronization phases must cancel in ρ_f, since the two diagrams are CP conjugates of one another, and the strong interactions are CP invariant. We therefore obtain $\rho_f = \exp(-2i\delta)$. And, from $\left|\rho_f\right| = 1$ we get,

$$\mathrm{Im}\,\bar{\alpha}_f = -\,\mathrm{Im}\,\alpha_f. \tag{44}$$

Equation (44) holds for any decay to a **CP-eigenstate that is described by a single weak amplitude**. Thus, for this class of final states we have (using eqs. (15) and (37)),

$$\Gamma(\overset{(-)}{B}{}^0_q(t) \to \overset{(-)}{f}) \;\; = \left|\langle f|B_q^0\rangle\right|^2 e^{-t/\tau}\left[1 \mp \mathrm{Im}\,\alpha_f \sin x_q \tfrac{t}{\tau}\right] \tag{45}$$

Now, the asymmetry (36) assumes the elegantly simple form (first given in [49]),

$$A_f(t) = -\,\mathrm{Im}\,\alpha_f \sin x_q \frac{t}{\tau} \; . \tag{46}$$

Further details for this case are given in sec. 2.5.

2.3.4 Time Dependence of the Decay of an Entangled B^0-$\bar{B}^0$ Pair

The quantum correlations first discussed by Einstein, Podolsky and Rosen [74] arise when B^0 and $\bar{B}^0$ meson are produced at time $t = 0$ in an entangled state of definite CP, $(|B_1^0\rangle|\bar{B}_2^0\rangle \pm |\bar{B}_1^0\rangle|B_1^0\rangle)/\sqrt{2}$, where the $+(-)$ sign is for the CP-even(odd) state, and indices 1,2 refer to the particles of momenta $\mathbf{P}_1$ and $\mathbf{P}_2$.

In the remainder of this note, time is measured in units of the B-lifetime.

Application to B_d^0 Mixing

We first consider the case that both mesons decay to a state $g \neq \bar{g}$ (such as $e\nu X$, $\bar{g} = e^-\bar{\nu}_e\bar{X}$) via a single weak amplitude that allows a determination as to whether each meson was a B^0 or $\bar{B}^0$ at the times t_1 and t_2 of their decays (as in the experiment [27] which measured the mixing parameter x_d.). A quantity of interest here is the ratio of the number of events where B_1 and B_2 both decay to g or both to $\bar{g}$ (which can only occur as an effect of B^0-$\bar{B}$ mixing) to the number of events where one meson decays to g and the other to $\bar{g}$,

$$r = \frac{N(B_1^0 \to g, B_2^0 \to g) + N(\bar{B}_1^0 \to \bar{g}, \bar{B}_2^0 \to \bar{g})}{N(B_1^0 \to g, \bar{B}_2^0 \to \bar{g}) + N(B_1^0 \to g, \bar{B}_2^0 \to \bar{g})}\,, \tag{47}$$

Recalling eqs. (16)-(17), the time evolution of the entangled initial state is given by,

$$|B_1^0\rangle|\bar{B}_2^0\rangle \quad\to\quad \left(F_+(t_1)|B_1^0\rangle + \frac{q}{p}F_-(t_1)|\bar{B}_1^0\rangle\right)\left(\frac{p}{q}F_-(t_2)|B_2^0\rangle + F_+(t_2)|\bar{B}_2^0\rangle\right), \tag{48}$$

$$|\bar{B}_1^0\rangle|B_2^0\rangle \quad\to\quad \left(\frac{p}{q}F_-(t_1)|B_1^0\rangle + F_+(t_1)|\bar{B}_1^0\rangle\right)\left(F_+(t_2)|B_2^0\rangle + \frac{q}{p}F_-(t_2)|\bar{B}_2^0\rangle\right), \tag{49}$$

$$\begin{aligned}
\frac{|B_1^0\rangle|\bar{B}_2^0\rangle \pm |\bar{B}_1^0\rangle|B_2^0\rangle}{\sqrt{2}} \quad\to\quad & \frac{p}{q}[F_+(t_1)F_-(t_2) \pm F_-(t_1)F_+(t_2)]\frac{|B_1^0\rangle|B_2^0\rangle}{\sqrt{2}} \\
& +[F_+(t_1)F_+(t_2) \pm F_-(t_1)F_-(t_2)]\frac{|B_1^0\rangle|\bar{B}_2^0\rangle}{\sqrt{2}} \\
& +[F_-(t_1)F_-(t_2) \pm F_+(t_1)F_+(t_2)]\frac{|\bar{B}_1^0\rangle|B_2^0\rangle}{\sqrt{2}} \\
& +\frac{q}{p}[F_-(t_1)F_+(t_2) \pm F_+(t_1)F_-(t_2)]\frac{|\bar{B}_1^0\rangle|\bar{B}_2^0\rangle}{\sqrt{2}} \\
& = e^{iM(t_1+t_2)}\, e^{-(t_1+t_2)/2}\Big\{\pm\frac{ip}{q}\sin\frac{x(t_1 \pm t_2)}{2}\frac{|B_1^0\rangle|B_2^0\rangle}{\sqrt{2}} \\
& +\cos\frac{x(t_1 \pm t_2)}{2}\frac{|B_1^0\rangle|\bar{B}_2^0\rangle}{\sqrt{2}} \pm \cos\frac{x(t_1 \pm t_2)}{2}\frac{|\bar{B}_1^0\rangle|B_2^0\rangle}{\sqrt{2}} \\
& +\frac{iq}{p}\sin\frac{x(t_1 \pm t_2)}{2}\frac{|\bar{B}_1^0\rangle|\bar{B}_2^0\rangle}{\sqrt{2}}\Big\}.
\end{aligned} \tag{50}$$

Note that the amplitudes vanish for the combinations of two like particles, $|B_1^0\rangle|B_2^0\rangle$ and $|\bar{B}_1^0\rangle|\bar{B}_2^0\rangle$, at times $t_1 = t_2$ if the B^0-$\bar{B}^0$ is produced in a CP-odd state. Such persistence of the initial quantum correlation for spacelike-separated events puzzled Einstein, Podolsky and Rosen, and remains ever impressive.

With the good assumption that the total decay rates obey $\Gamma[\bar{B}^0 \to \bar{g}] = \Gamma[B^0 \to g]$, the time dependences of the rates for decays are,

$$
\begin{aligned}
&\Gamma[B_1^0(t_1) \to g]\, \Gamma[B_2^0(t_2) \to g] = \left| \frac{p}{q}[F_+(t_1)F_-(t_2) \pm F_-(t_1)F_+(t_2)] \frac{\langle g|B_1^0\rangle \langle g|B_2^0\rangle}{\sqrt{2}} \right|^2 \\
&= \sin^2 \frac{xt_1 \pm x_2 t_2}{2} \frac{e^{-(t_1+t_2)}\Gamma^2[B^0 \to g]}{2}\,, \qquad (51) \\
&\Gamma[\bar{B}_1^0(t_1) \to \bar{g}]\, \Gamma[\bar{B}_2^0(t_2) \to \bar{g}] = \left| \frac{q}{p}[F_-(t_1)F_+(t_2) \pm F_+(t_1)F_-(t_2)] \frac{\langle \bar{g}|\bar{B}_1^0\rangle \langle \bar{g}|\bar{B}_2^0\rangle}{\sqrt{2}} \right|^2 \\
&= \Gamma[B_1^0(t_1) \to g]\, \Gamma[B_2^0(t_2) \to g], \qquad (52) \\
&\Gamma[B_1^0(t_1) \to g]\, \Gamma[\bar{B}_2^0(t_2) \to \bar{g}] = \left| [F_+(t_1)F_+(t_2) \pm F_-(t_1)F_-(t_2)] \frac{\langle g|B_1^0\rangle \langle \bar{g}|\bar{B}_2^0\rangle}{\sqrt{2}} \right|^2 \\
&= \cos^2 \frac{xt_1 \pm x_2 t_2}{2} \frac{e^{-(t_1+t_2)}\Gamma^2[B^0 \to g]}{2}\,, \qquad (53) \\
&\Gamma[\bar{B}_1^0(t_1) \to \bar{g}]\, \Gamma[B_2^0(t_2) \to g] = \left| [F_-(t_1)F_-(t_2) \pm F_+(t_1)F_+(t_2)] \frac{\langle \bar{g}|\bar{B}_1^0\rangle \langle g|B_2^0\rangle}{\sqrt{2}} \right|^2 \\
&= \Gamma[B_1^0(t_1) \to g]\, \Gamma[\bar{B}_2^0(t_2) \to \bar{g}]. \qquad (54)
\end{aligned}
$$

Note that

$$
\begin{aligned}
&\Gamma[B_1^0(t_1) \to g]\, \Gamma[B_2^0(t_2) \to g] + \Gamma[\bar{B}_1^0(t_1) \to \bar{g}]\, \Gamma[\bar{B}_2^0(t_2) \to \bar{g}] + \Gamma[B_1^0(t_1) \to g]\, \Gamma[\bar{B}_2^0(t_2) \to \bar{g}] \\
&+\Gamma[\bar{B}_1^0(t_1) \to \bar{g}]\, \Gamma[B_2^0(t_2) \to g] = e^{-(t_1+t_2)}\Gamma^2[B^0 \to g], \qquad (55)
\end{aligned}
$$

and that B_1 and B_2 cannot both decay to g (or to $\bar{g}$) at the same time $t_1 = t_2$ if they are in a CP-odd state.

For a total of N_0 produced B^0-$\bar{B}^0$ pairs, the numbers of observed decay combinations would be,

$$
\begin{aligned}
&N(B_1^0 \to g, B_2^0 \to g) = N(\bar{B}_1^0 \to \bar{g}, \bar{B}_2^0 \to \bar{g}) \\
&= N_0 \int_0^\infty dt_1 \int_0^\infty dt_2 \left[\cos^2 \frac{xt_1}{2} \sin^2 \frac{xt_2}{2} + \sin^2 \frac{xt_1}{2} \cos^2 \frac{xt_2}{2} \pm 2\cos\frac{xt_1}{2} \sin\frac{xt_1}{2} \cos\frac{xt_2}{2} \sin\frac{xt_2}{2} \right] \\
&\quad \frac{e^{-(t_1+t_2)}\Gamma^2[B^0 \to g]}{2} = \frac{N_0\Gamma^2[B^0 \to g]}{4} \frac{x^2(2 \pm 1 + x^2)}{(1+x^2)^2}\,, \qquad (56) \\
&N(B_1^0 \to g, \bar{B}_2^0 \to \bar{g}) = N(\bar{B}_1^0 \to \bar{g}, B_2^0 \to g) \\
&= N_0 \int_0^\infty dt_1 \int_0^\infty dt_2 \left[\cos^2 \frac{xt_1}{2} \cos^2 \frac{xt_2}{2} + \sin^2 \frac{xt_1}{2} \sin^2 \frac{xt_2}{2} \mp 2\cos\frac{xt_1}{2} \sin\frac{xt_1}{2} \cos\frac{xt_2}{2} \sin\frac{xt_2}{2} \right] \\
&\quad \frac{e^{-(t_1+t_2)}\Gamma^2[B^0 \to g]}{2} = \frac{N_0\Gamma^2[B^0 \to g]}{4} \frac{2 + x^2(2 \mp 1 + x^2)}{(1+x^2)^2}\,. \qquad (57)
\end{aligned}
$$

As expected,

$$
\begin{aligned}
&N(B_1^0 \to g, B_2^0 \to g) + N(\bar{B}_1^0 \to \bar{g}, \bar{B}_2^0 \to \bar{g}) + N(B_1^0 \to g, \bar{B}_2^0 \to \bar{g}) + N(B_1^0 \to g, \bar{B}_2^0 \to \bar{g}) \\
&= N_0\Gamma^2[B^0 \to g]. \qquad (58)
\end{aligned}
$$

Then, (as in the Appendix of [62] with y = 0),

$$r = \frac{N(B_1^0 \to g, B_2^0 \to g) + N(\bar{B}_1^0 \to \bar{g}, \bar{B}_2^0 \to \bar{g})}{N(B_1^0 \to g, \bar{B}_2^0 \to \bar{g}) + N(B_1^0 \to g, \bar{B}_2^0 \to \bar{g})} = \frac{x^2(2 \pm 1 + x^2)}{2 + x^2(2 \mp 1 + x^2)}\,, \tag{59}$$

which has nontrivial dependence on x for the B_d^0-$\bar{B}_d^0$ system (but not for the B_s^0-$\bar{B}_s^0$ system where $x_s \gg 1$).

Application to Method 4

We next consider the case that meson B_1 decays to a CP-eigenstate f at time t_1 (in units of the B-lifetime) as in method 4 for the study of CP violation in the B^0-$\bar{B}^0$ system, while meson B_2 decays to a state $g \neq \bar{g}$ (such as $g = e^+\nu_e X$) via a single weak amplitude that allows a determination as to whether the second meson was a B^0 or $\bar{B}^0$ at the time t_2 of its decay. The CP-violating decay asymmetry is then [50, 62],

$$A(t_1, t_2) = \frac{\Gamma[B_1(t_1) \to f]\,\Gamma[\bar{B}_2^0(t_2) \to \bar{g}] - \Gamma[B_1(t_1) \to f]\,\Gamma[B_2^0(t_2) \to g]}{\Gamma[B_1(t_1) \to f]\,\Gamma[\bar{B}_2^0(t_2) \to \bar{g}] + \Gamma[B_1(t_1) \to f]\,\Gamma[B_2^0(t_2) \to g]}\,. \tag{60}$$

where B_1 could be either B_1^0 or $\bar{B}_1^0$.

Recalling eqs. (48)-(50), the products of the decay rates are,

$$\begin{aligned}
\Gamma[B_1(t_1) \to f]\,\Gamma[\bar{B}_2^0(t_2) \to \bar{g}] &= \Bigg|[F_+(t_1)F_+(t_2) \pm F_-(t_1)F_-(t_2)]\frac{\langle f|B_1^0\rangle\langle \bar{g}|\bar{B}_2^0\rangle}{\sqrt{2}} \\
&\qquad + \frac{q}{p}[F_-(t_1)F_+(t_2) \pm F_+(t_1)F_-(t_2)]\frac{\langle f|\bar{B}_1^0\rangle\langle \bar{g}|\bar{B}_2^0\rangle}{\sqrt{2}}\Bigg|^2, \\
&= \left|\cos\frac{x(t_1 \pm t_2)}{2} + \frac{iq}{p}\frac{\langle f|\bar{B}_1^0\rangle}{\langle f|B_1^0\rangle}\sin\frac{x(t_1 \pm t_2)}{2}\right|^2 \frac{e^{-(t_1+t_2)}\Gamma[B^0 \to f]\,\Gamma[\bar{B}^0 \to \bar{g}]}{2} \\
&= [1 + \sin 2\varphi \sin(xt_1 \pm xt_2)]\,\frac{e^{-(t_1+t_2)}\Gamma[B^0 \to f]\,\Gamma[B^0 \to g]}{2}\,,
\end{aligned} \tag{61}$$

where 2φ is the phase of the ratio $q\langle f|\bar{B}_1^0\rangle/p\langle f|B_1^0\rangle = \alpha_f = e^{2i\varphi}$ (recalling eqs. (38)-(39)), and we have assumed that $\Gamma[\bar{B}^0 \to \bar{g}] = \Gamma[B^0 \to g]$. Similarly,

$$\begin{aligned}
\Gamma[B_1(t_1) \to f]\,\Gamma[B_2^0(t_2) \to g] &= \Bigg|\frac{p}{q}[F_+(t_1)F_-(t_2) \pm F_-(t_1)F_+(t_2)]\frac{\langle f|B_1^0\rangle\langle g|B_2^0\rangle}{\sqrt{2}} \\
&\qquad + [F_-(t_1)F_-(t_2) \pm F_+(t_1)F_+(t_2)]\frac{\langle f|\bar{B}_1^0\rangle\langle g|B_2^0\rangle}{\sqrt{2}}\Bigg|^2, \\
&= \left|\frac{ip}{q}\frac{\langle f|B_1^0\rangle}{\langle f|\bar{B}_1^0\rangle}\sin\frac{x(t_1 \pm t_2)}{2} + \cos\frac{x(t_1 \pm t_2)}{2}\right|^2 \frac{e^{-(t_1+t_2)}\Gamma[B^0 \to f]\,\Gamma[B^0 \to g]}{2} \\
&= [1 - \sin 2\varphi \sin(xt_1 \pm xt_2)]\,\frac{e^{-(t_1+t_2)}\Gamma[B^0 \to f]\,\Gamma[B^0 \to g]}{2}\,,
\end{aligned} \tag{62}$$

noting that $p\langle f|B_1^0\rangle/q\langle f|\bar{B}_1^0\rangle = \bar{\alpha}_f = e^{-2i\varphi}$ so $\mathrm{Re}(ip\langle f|B_1^0\rangle/q\langle f|\bar{B}_1^0\rangle) = -\sin 2\varphi$. Thus, the decay asymmetry is,

$$A(t_1, t_2) = \sin 2\varphi \sin(xt_1 \pm xt_2). \tag{63}$$

If both B's decay at the same time, one must be a B^0 and the other a $\bar{B}^0$, and there can be no decay asymmetry at such times, since $\Gamma[B^0 \to f]\,\Gamma[\bar{B}^0 \to \bar{g}] = \Gamma[\bar{B}^0 \to f]\,\Gamma[B^0 \to g]$. But, when decay time t_1 differs from t_2, the particle can have mixed into any of the four combinations $B_1^0 B_2^0$, $\bar{B}_1^0 B_2^0$, $B_1^0 \bar{B}_2^0$ and $\bar{B}_1^0 \bar{B}_2^0$, and the interference among the four decay amplitudes leads to a nonzero decay asymmetry.

If the detector cannot determine the decay times t_1 and t_2, it could still observe the time-integrated decay rates,

$$
\begin{aligned}
&\int_0^\infty \int_0^\infty \Gamma[B_1(t_1) \to f]\,\Gamma[\bar{B}_2^0(t_2) \to \bar{g}]\,dt_1\,dt_2 = \\
&= \int_0^\infty \int_0^\infty (1 + \sin 2\varphi \sin(xt_1 \pm xt_2))\,\frac{e^{-(t_1+t_2)}\Gamma[B^0 \to f]\,\Gamma[B^0 \to g]}{2}\,dt_1\,dt_2 \\
&= \left(1 + \sin 2\varphi \frac{x^2(1 \pm 1)}{(1+x^2)^2}\right) \frac{\Gamma[B^0 \to f]\,\Gamma[B^0 \to g]}{2}\,,
\end{aligned}
\tag{64}
$$

$$
\begin{aligned}
&\int_0^\infty \int_0^\infty \Gamma[B_1(t_1) \to f]\,\Gamma[B_2^0(t_2) \to \bar{g}]\,dt_1\,dt_2 = \\
&= \int_0^\infty \int_0^\infty (1 - \sin 2\varphi \sin(xt_1 \pm xt_2))\,\frac{e^{-(t_1+t_2)}\Gamma[B^0 \to f]\,\Gamma[B^0 \to g]}{2}\,dt_1\,dt_2 \\
&= \left(1 - \sin 2\varphi \frac{x^2(1 \pm 1)}{(1+x^2)^2}\right) \frac{\Gamma[B^0 \to f]\,\Gamma[B^0 \to g]}{2}\,,
\end{aligned}
\tag{65}
$$

and the time-integrated asymmetry would be,

$$
A = (1 \pm 1) \sin 2\varphi \frac{x}{(1+x^2)^2}\,,
\tag{66}
$$

which vanishes if the B's were produced in a CP-odd state, as occurs at an e^+e^- collider operated at the $\Upsilon(4S)$ resonance, where the B-production rate is maximal. In this case, the B's are so slowly moving in the laboratory that their decay times cannot be resolved, and measurements of CP violation could not be made. To avoid this limitation, so-called asymmetric e^+e^- colliders were built, following a suggestion by Oddone [75], such that the e^+e^- center of mass has sufficient velocity in the lab that the decay points of both mesons B_1 and B_2 can be reconstructed, and time-dependent analyses performed, as in [9, 10].

We can say that the Einstein-Podolsky-Rosen effect required that asymmetric e^+e^- colliders to be built for CP violation to be observable in the B^0-$\bar{B}^0$ system.

2.4 Method 1: B Decays to D^0X, $\bar{D}^0X$, and $D^0_{1,2}X$ where $X \neq \bar{X}$

When a B meson (*i.e.*, one that contains a $\bar{b}$-quark) decays to $\bar{D}^0X$ via a spectator graph (graphs I and II of Fig. 6 in Appendix A) this involves a $\bar{b} \to \bar{c}$ transition, and hence no weak phase:

$$
A(B \to \bar{D}^0 X) = \left|A_{\bar{f}}\right| e^{i\delta_{\bar{f}}},
\tag{67}
$$

where $\delta_{\bar{f}}$ is a final-state strong-interaction phase. But when a B meson decays to D^0X this involves the transition $\bar{b} \to \bar{u}$ and hence the weak phase $-\phi_{ub}$ appears in the amplitude,

$$A(B \to D^0X) = |A_f|\, e^{-i\phi_{ub}} e^{i\delta_f}, \tag{68}$$

The two amplitudes A_f and $A_{\bar{f}}$ interfere when the D forms one of the CP eigenstates $D^0_{1,2} = (D^0 \pm \bar{D}^0)/\sqrt{2}$,

$$A(B \to D^0_{1,2}X) = (|A_f|\, e^{-i\phi_{ub}} e^{i\delta_f} \pm \left|A_{\bar{f}}\right| e^{i\delta_{\bar{f}}})/\sqrt{2}. \tag{69}$$

In eqs. (67-68) we have supposed that all graphs contributing to each decay have the same weak phases (which is not necessarily true, as discussed below).

When $X \neq \bar{X}$ the decays are self-tagging as to whether the parent was a B or a $\bar{B}$. Then, even for neutral B's there is no effect due to mixing on the observed decay rates. Method 1 could be used at a symmetric e^+e^- collider without the penalty due to mixing of methods 2-6.

Assuming equal production rates for B and $\bar{B}$ the decay rates are proportional to the number of decays observed. We can therefore measure,

$$\begin{aligned}
\Gamma(B \to \bar{D}^0X) = \Gamma(\bar{B} \to D^0\bar{X}) \quad &\propto \left|A_{\bar{f}}\right|^2, \\
\Gamma(B \to D^0X) = \Gamma(\bar{B} \to \bar{D}^0\bar{X}) \quad &\propto |A_f|^2, \\
\Gamma(B \to D^0_{1,2}X) \quad &\propto (\left|A_{\bar{f}}\right|^2 + |A_f|^2)/2 \pm \left|A_{\bar{f}}\right| |A_f| \cos(\phi_{ub} + \delta), \\
\Gamma(\bar{B} \to D^0_{1,2}\bar{X}) \quad &\propto (\left|A_{\bar{f}}\right|^2 + |A_f|^2)/2 \pm \left|A_{\bar{f}}\right| |A_f| \cos(\phi_{ub} - \delta),
\end{aligned} \tag{70}$$

recalling eq. (30), and defining $\delta = \delta_{\bar{f}} - \delta_f$ as the strong-interaction phase difference.

Thus there are eight possible measurements depending on the four quantities $\left|A_{\bar{f}}\right|$, $|A_f|$, $\cos(\phi_{ub} + \delta)$ and $\cos(\phi_{ub} - \delta)$. Therefore we can deduce $|\phi_{ub} \pm \delta|$ and hence determine ϕ_{ub} up to a fourfold ambiguity,

$$\phi_{ub} = \frac{\pm |\phi_{ub} + \delta| \pm |\phi_{ub} - \delta|}{2}. \tag{71}$$

The strong phase difference δ depends on the particular final state D^0X studied, so if these measurements can be carried out for different X the discrete ambiguity may be removable.

In contrast to sec. 2.3.1 where only two rate measurements were considered, the use of 4-8 measurements in the present method permits ϕ_{ub} to be determined whether on not the strong interaction phase difference δ is nonvanishing. Indeed, it would be preferable if δ were zero, as the discrete ambiguity is only twofold in this case.

We now consider examples of particular decay modes that might be used to implement this procedure. First, we consider the question of identifying the CP eigenstates $D^0_{1,2}$. From Table 8 of Appendix A in which the basic two-body decays of the D^0 are listed we infer that the CP(even) state D^0_1 can decay according to,

$$D^0_1 \to \pi^+\pi^-,\ K^+K^-,\ K^0_SK^0_S,\ K^0_LK^0_L,\ K^0_L\pi^0,\ K^0_L\eta,\ K^0_L\rho^0,\ K^0_L\omega,\ K^0_L\phi,\ etc. \tag{72}$$

and the CP-odd state D_2^0 can decay to,

$$D_2^0 \to K_S^0\pi^0,\ K_S^0\eta,\ K_S^0K_L^0,\ K_S^0\rho^0,\ K_S^0\omega,\ K_S^0\phi,\ etc. \tag{73}$$

Several of the decays of the D_2^0 have been observed, and the fraction of D^0's that decay as D_2^0 is at least 2%. However, all D_2^0 decays except $K_S^0\rho^0 \to \pi^+\pi^-\pi^+\pi^-$ and $K_S^0\phi \to \pi^+\pi^-K^+K^-$ involve at least two final-state photons. If we suppose that only all-charged final-states will be reconstructed at a hadron collider, then only about 0.5% of all D^0's will decay to identifiable D_2^0 modes. The D_1^0 decays predominantly to all-charged daughters, but again only about 0.5% of all D^0's will decay to identifiable D_1^0 modes. In sum, about 2-5% of D^0's might be usable for the $D_{1,2}^0$ analysis at an e^+e^- collider, but only about 1% at a hadron collider.

In principle, the decays $B \to D^{\star 0}X$ decays are also usable for the present analysis as $D_{1,2}^{\star 0} = (D^{\star 0} \pm \bar{D}^{\star 0})/\sqrt{2}$ are CP(even) and (odd) eigenstates, respectively. However, in the decays $D^{\star 0} \to D^0\pi^0$ and $D^0\gamma$ the final-state orbital angular momentum is one in both cases and so the CP eigenstates decay according to,

$$D_1^{\star 0} \to D_1^0\pi^0, \qquad \text{but} \qquad D_1^{\star 0} \to D_2^0\gamma, \qquad etc. \tag{74}$$

Hence, the $D_{1,2}^{\star 0}$ states can only be correctly identified if the single γ can be distinguished from the π^0. As both the γ and π^0 are quite soft this may be possible at an e^+e^- collider but is problematic at a hadron collider.

Finally we consider specific B-decay modes that are suitable for method 1. Referring to Tables 2-5 in Appendix A, we find the following candidates,

$$\begin{aligned}
B_u^+ &\to \left\{\begin{array}{ll} \bar{D}^0\pi^+ & [\mathrm{I}_F, \mathrm{II}_F] \\ D^0\pi^+ & [\mathrm{II}_D, \mathrm{III}_D] \end{array}\right. , \qquad \left\{\begin{array}{ll} \bar{D}^0K^+ & [\mathrm{I}_S, \mathrm{II}_S] \\ D^0K^+ & [\mathrm{II}_S, \mathrm{III}_S] \end{array}\right. , \\
B_d^0 &\to \left\{\begin{array}{ll} \bar{D}^0K^{\star 0} & [\mathrm{II}_S] \\ D^0K^{\star 0} & [\mathrm{II}_S] \end{array}\right. , \\
B_s^0 &\to \left\{\begin{array}{ll} \bar{D}^0K^{\star 0} & [\mathrm{II}_F] \\ D^0K^{\star 0} & [\mathrm{II}_D] \end{array}\right. , \\
B_c^+ &\to \left\{\begin{array}{ll} \bar{D}^0D^+ & [\mathrm{II}_F, \mathrm{III}_F] \\ D^0D^+ & [\mathrm{I}_D, \mathrm{II}_D] \end{array}\right. , \qquad \left\{\begin{array}{ll} \bar{D}^0D_s^+ & [\mathrm{II}_S, \mathrm{III}_S] \\ D^0D_s^+ & [\mathrm{I}_S, \mathrm{II}_S] \end{array}\right. .
\end{aligned} \tag{75}$$

The Roman numerals refer to the type of graph, as shown in Fig. 6 of Appendix A, and the subscripts F, S, and D refer to CKM-favored (order λ^2), -suppressed (order λ^3), and -doubly-suppressed (order λ^4), respectively. In addition, b-baryons have suitable modes, such as Λ_b^0 $(udb) \to \Lambda D^0(\bar{D}^0)$, Λ_b^+ $(udb) \to \Sigma^+D^0(\bar{D}^0)$, Σ_b^0 $(usb) \to \Xi^0D^0(\bar{D}^0)$, *etc.* [57], which we will not discuss further.

Among the candidate B-meson decays, only $B_d^0 \to D^0(\bar{D}^0)K^{\star 0}$ is ideally suited for method 1, as only one graph contributes to each decay and these are both singly CKM-suppressed type-II (color-suppressed) spectator graphs. These decays have not yet been observed, but should have branching ratios of order 10^{-5}. If only about 1% of the decays are useful for the $D^0_{1,2}$ analysis, the effective branching ratio is about 10^{-7}. So at least 10^9 B's must be produced to carry out method 1. Some advantage is gained by considering several channels, but since the strong phase difference varies from channel to channel, there must be enough events in each channel to carry out the analysis separately before results for ϕ_{ub} can be combined. Hence, method 1 may be out of range of e^+e^- B factories with luminosity of 3×10^{33} cm^{-2}sec^{-1}, even though the method is well-suited in principle to them.

The other five candidate decay pairs listed above all suffer from the rate for D^0X being at least an order of magnitude less than that for $\bar{D}^0X$ (or *vice versa*), so the interference term in $D^0_{1,2}X$ is quite small. However, the branching fraction for $B^+ \to D^0K^+$ is likely to be very similar to that for $B^0_d \to D^0K^{\star 0}$. Since the statistical accuracy of method 1 is largely set by the number of events of whichever of D^0X or $\bar{D}^0X$ has the lower branch, we conclude that $B^+ \to D^0(\bar{D}^0)K^+$ is about as useful as $B^0_d \to D^0(\bar{D}^0)K^{\star 0}$.

If B_c mesons were produced as copiously as B^+ and B^0_d then the decay pair $B^+_c \to D^0(\bar{D}^0)D^+_s$ would be also be useful. However, B_c production is likely to be suppressed at both e^+e^- and hadron colliders.

2.5 Method 2: Neutral B-Meson Decays to f and $\bar{f}$ where $f \neq \bar{f}$

In the second method the needed interference arises from mixing of a B^0 and $\bar{B}^0$. The analysis is more straightforward if the final state f is not self conjugate ($f \neq \bar{f}$), but then both the B^0 and $\bar{B}^0$ must decay to both f and $\bar{f}$.

As for decay pairs suitable for method 1, one of the decay pairs (here called $\bar{f}$) proceeds via a $\bar{b} \to \bar{c}$ transition, and the other (f) via $\bar{b} \to \bar{u}$. So we may write,

$$\begin{aligned} A(B^0 \to \bar{f}) &= \left|A_{\bar{f}}\right| e^{i\delta_{\bar{f}}}, \\ A(B^0 \to f) &= \left|A_f\right| e^{-i\phi_{ub}} e^{i\delta_f}, \\ A(\bar{B}^0 \to f) &= \left|A_{\bar{f}}\right| e^{i\delta_{\bar{f}}}, \\ A(\bar{B}^0 \to \bar{f}) &= \left|A_f\right| e^{i\phi_{ub}} e^{i\delta_f}, \end{aligned} \tag{76}$$

using eq. (30). In writing this we must be able to assume that each amplitude is dominated by a single weak phase.

Due to mixing, a particle that was created as a B^0 (or $\bar{B}^0$) at $t = 0$ has evolved by time t to the state we label as $B^0(t)$ (or $\bar{B}^0(t)$) according to,

$$\begin{aligned} B^0(t) &= e^{-iMt} e^{-t/2} [\cos(xt/2)|B^0\rangle + i e^{2i\phi_M} \sin(xt/2)|\bar{B}^0\rangle], \\ \bar{B}^0(t) &= e^{-iMt} e^{-t/2} [i e^{-2i\phi_M} \sin(xt/2)|B^0\rangle + \cos(xt/2)|\bar{B}^0\rangle], \end{aligned} \tag{77}$$

where throughout this paper we measure time in units of the relevant B lifetime, $x = \Delta M/\Gamma$ is the mixing parameter, and the relative amount of $|B^0\rangle$ and $|\bar{B}^0\rangle$ in the weak eigenstate B^0_S is given by a pure phase coming from the box diagram [11], where,

$$\phi_M = \begin{cases} \phi_{td}, & \text{for } B^0_d \\ \phi_{ts} \approx 0, & \text{for } B^0_s \end{cases} \tag{78}$$

The four time-dependent decay rates are then,

$$\begin{aligned}
\Gamma(B^0(t)\to\bar f) &\propto e^{-t}[\left|A_{\bar f}\right|^2\cos^2(xt/2)+|A_f|^2\sin^2(xt/2)-\overline{S}\sin(xt)],\\
\Gamma(B^0(t)\to f) &\propto e^{-t}[|A_f|^2\cos^2(xt/2)+\left|A_{\bar f}\right|^2\sin^2(xt/2)-S\sin(xt)],\\
\Gamma(\bar B^0(t)\to f) &\propto e^{-t}[\left|A_{\bar f}\right|^2\cos^2(xt/2)+|A_f|^2\sin^2(xt/2)+S\sin(xt)],\\
\Gamma(\bar B^0(t)\to\bar f) &\propto e^{-t}[|A_f|^2\cos^2(xt/2)+\left|A_{\bar f}\right|^2\sin^2(xt/2)+\overline{S}\sin(xt)],
\end{aligned}\tag{79}$$

where $\delta=\delta_{\bar f}-\delta_f$ is the strong-interaction phase difference, and

$$\overline{S}=|A_f|\left|A_{\bar f}\right|\sin(2\phi_M+\phi_{ub}-\delta),\qquad\text{and}\qquad S=|A_f|\left|A_{\bar f}\right|\sin(2\phi_M+\phi_{ub}+\delta).\tag{80}$$

For eventual Fourier analysis it is preferable to write eqs. (79) as,

$$\begin{aligned}
\Gamma(B^0(t)\to\bar f) &\propto e^{-t}[K+C\cos(xt)-\overline{S}\sin(xt)],\\
\Gamma(B^0(t)\to f) &\propto e^{-t}[K-C\cos(xt)-S\sin(xt)],\\
\Gamma(\bar B^0(t)\to f) &\propto e^{-t}[K+C\cos(xt)+S\sin(xt)],\\
\Gamma(\bar B^0(t)\to\bar f) &\propto e^{-t}[K-C\cos(xt)+\overline{S}\sin(xt)],
\end{aligned}\tag{81}$$

where,

$$K=(\left|A_{\bar f}\right|^2+|A_f|^2)/2,\qquad\text{and}\qquad C=(\left|A_{\bar f}\right|^2-|A_f|^2)/2.\tag{82}$$

From measurement of these four time-dependent decay rates one deduces the four quantities $|A_f|$, $\left|A_{\bar f}\right|$, $\sin(2\phi_M+\phi_{ub}+\delta)$, and $\sin(2\phi_M+\phi_{ub}-\delta)$. Thus, we can measure $|\pi/2-2\phi_M-\phi_{ub}\pm\delta|$, and thereby determine $2\phi_M+\phi_{ub}$ up to a fourfold ambiguity,

$$2\phi_M+\phi_{ub}=\frac{\pi\pm|\pi/2-2\phi_M-\phi_{ub}+\delta|\pm|\pi/2-2\phi_M-\phi_{ub}\pm\delta|}{2}.\tag{83}$$

As for method 1, the use of four rate measurements permits the weak phase $2\phi_M+\phi_{ub}$ to be extracted even when the strong phase difference δ vanishes.

To carry out the above analysis we must know for each decay whether the B was created as a B^0 or a $\bar B^0$. The decays are not self tagging since both B^0 and $\bar B^0$ can decay to both f and $\bar f$, so in method 2 (as well as methods 3-6) one must tag the particle/antiparticle character of the second B in the event. As that B may also be subject to mixing, a dilution of the statistical power of the method results. In particular, it is well-known that at an e^+e^- collider when the B-$\bar B$ pair is produced in a C-odd state the interesting terms in $\sin(xt)$ in eqs. (83) cannot be measured unless the B's have relativistic velocity in the lab frame. This "penalty" due to mixing can only be overcome by use of an asymmetric e^+e^- collider if the center-of-mass energy is that of the $\Upsilon(4S)$.

From Tables 3 and 4 of Appendix A we find that there are 4 candidate decays pairs for implementing method 2,

$$\begin{aligned}
B_d^0\to &\left\{\begin{array}{ll} D^-\pi^+ & [\mathrm{I}_F,\ \mathrm{IV}_F]\\ D^+\pi^- & [\mathrm{I}_D,\ \mathrm{IV}_D]\end{array}\right., &&\left\{\begin{array}{ll} D_s^-K^+ & [\mathrm{IV}_F]\\ D_s^+K^- & [\mathrm{IV}_D]\end{array}\right.,\\
B_s^0\to &\left\{\begin{array}{ll} D_s^-K^+ & [\mathrm{I}_S,\ \mathrm{IV}_S]\\ D_s^+K^- & [\mathrm{I}_S,\ \mathrm{IV}_S]\end{array}\right., &&\left\{\begin{array}{ll} D^-\pi^+ & [\mathrm{IV}_S]\\ D^+\pi^- & [\mathrm{IV}_S]\end{array}\right.,
\end{aligned}\tag{84}$$

In each example the lower decay depends on the weak phase $-\phi_{ub}$. The type-IV W-exchange graphs (Fig. 6) may well be highly suppressed compared to the type-I spectator graphs. Thus of the four candidates, only $B_s^0 \to D_s^{\pm} K^{\mp}$ is likely to have reasonably large ($\sim 10^{-4}$) branching ratios for both channels. This renders method 2 largely unsuitable for an e^+e^- collider, where production of B_s mesons will be low. At a hadron collider where only all-charged daughters are used in reconstructing the B_s about 5-10% of the D_s decays will be useful. Accounting for dilutions due to mixing of the second B at a hadron collider, some 10^8-10^9 B_s are needed to implement method 2.

If method 2 is used for the decays $B_s^0 \to D_s^{\pm} K^{\mp}$ the weak phase that is measured in just ϕ_{ub}, since the mixing phase ϕ_M vanishes for B_s^0.

2.6 Method 3: Neutral B-Meson Decays to $D^0 X$, $\bar{D}^0 X$, and $D^0_{1,2} X$ where $X = \bar{X}$

Aspects of methods 1 and 2 are combined when a neutral B-meson decays to final state $D^0 X$ where X is self conjugate ($X = \bar{X}$). Now, interference arises both from mixing and from the use of $D^0_{1,2}$ channels.

Following eqs. (67-69) and (76), we write the eight related decay amplitudes as,

$$\begin{aligned}
A(B^0 \to \bar{D}^0 X) &= \left|A_{\bar{f}}\right| e^{i\delta_{\bar{f}}}, \\
A(B^0 \to D^0 X) &= \left|A_f\right| e^{-i\phi_{ub}} e^{i\delta_f}, \\
A(\bar{B}^0 \to D^0 X) &= \left|A_{\bar{f}}\right| e^{i\delta_{\bar{f}}}, \\
A(\bar{B}^0 \to \bar{D}^0 X) &= \left|A_f\right| e^{i\phi_{ub}} e^{i\delta_f}, \\
A(B^0 \to D^0_{1,2} X) &= (\left|A_f\right| e^{-i\phi_{ub}} e^{i\delta_f} \pm \left|A_{\bar{f}}\right| e^{i\delta_{\bar{f}}})/\sqrt{2} \equiv A_{1,2}, \\
A(\bar{B}^0 \to D^0_{1,2} X) &= (\left|A_{\bar{f}}\right| e^{i\delta_{\bar{f}}} \pm \left|A_f\right| e^{i\phi_{ub}} e^{i\delta_f})/\sqrt{2} \equiv \bar{A}_{1,2}.
\end{aligned} \tag{85}$$

Because both $D^0 X$ and $\bar{D}^0 X$ can be reached from both B^0 and $\bar{B}^0$, mixing must always be taken into account. In addition to the four time-dependent decay rates given in eq. (81), there are four more involving $D^0_{1,2}$ obtained by combining eqs. (77) and (85),

$$\begin{aligned}
\Gamma(B^0(t) \to D^0_{1,2} X) &\propto e^{-t}[\left|A_{1,2}\right|^2 \cos^2(xt/2) + \left|\bar{A}_{1,2}\right|^2 \sin^2(xt/2) - S_{1,2}\sin(xt)], \\
&= e^{-t}[K_{1,2} - C_{1,2}\cos(xt) - S_{1,2}\sin(xt)], \\
\Gamma(\bar{B}^0(t) \to D^0_{1,2} X) &\propto e^{-t}[\left|\bar{A}_{1,2}\right|^2 \cos^2(xt/2) + \left|A_{1,2}\right|^2 \sin^2(xt/2) + S_{1,2}\sin(xt)], \\
&= e^{-t}[K_{1,2} + C_{1,2}\cos(xt) + S_{1,2}\sin(xt)],
\end{aligned} \tag{86}$$

where

$$
\begin{aligned}
|A_{1,2}|^2 &= (|A_{\bar f}|^2 + |A_f|^2)/2 \pm |A_{\bar f}|\,|A_f|\cos(\phi_{ub}+\delta),\\
|\bar A_{1,2}|^2 &= (|A_{\bar f}|^2 + |A_f|^2)/2 \pm |A_{\bar f}|\,|A_f|\cos(\phi_{ub}-\delta),\\
K_{1,2} &= (|A_{\bar f}|^2 + |A_f|^2)/2 \pm |A_{\bar f}|\,|A_f|\cos\phi_{ub}\cos\delta,\\
C_{1,2} &= \pm |A_{\bar f}|\,|A_f|\sin\phi_{ub}\sin\delta,\\
S_{1,2} &= 2\,|A_f|\,|A_{\bar f}|\sin(2\phi_M+\phi_{ub})\cos\delta \pm |A_f|^2\sin 2(\phi_M+\phi_{ub}) \pm |A_{\bar f}|^2\sin 2\phi_M,
\end{aligned}
\tag{87}
$$

and $\delta = \delta_{\bar f} - \delta_f$ is the strong-interaction phase difference.

From analysis of the four time-dependent rates (81) we deduce $|A_f|$, $|A_{\bar f}|$, $\sin(2\phi_M + \phi_{ub}+\delta)$ and $\sin(2\phi_M+\phi_{ub}-\delta)$. Then, from the coefficients $K_{1,2}$ and $C_{1,2}$ of eqs. (86) we also extract $\cos\phi_{ub}\cos\delta$ and $\sin\phi_{ub}\sin\delta$. Finally, from the coefficient of $\sin(xt)$ we can extract $\sin(2\phi_M+\phi_{ub})\cos\delta$, $\sin 2(\phi_M+\phi_{ub})$ and $\sin 2\phi_M$.

Thus method 3 leads to the simultaneous measurement of ϕ_M, ϕ_{ub}, $\phi_M+\phi_{ub}$ and $2\phi_M+\phi_{ub}$. In case of B_d^0 mesons for which $\phi_M = \phi_{td}$ (see eq. (78)) ϕ_{td} and ϕ_{ub} and $\phi_{td}+\phi_{ub}$ are measured at once. It is remarkable that all three of the phase angles of the unitarity triangle can be extracted from the analysis of a single family of B_d^0-decays.

From Tables 3 and 4 of Appendix A we find that there are six candidate decays pairs for implementing method 3,

$$
\begin{aligned}
B_d^0 \to &\left\{\begin{array}{ll}\bar D^0 K^0_{S,L} & [\mathrm{II}_S]\\ D^0 K^0_{S,L} & [\mathrm{II}_S]\end{array}\right., \quad
\left\{\begin{array}{ll}\bar D^0 \rho^0 & [\mathrm{II}_F,\ \mathrm{IV}_F]\\ D^0 \rho^0 & [\mathrm{II}_D,\ \mathrm{IV}_D]\end{array}\right., \quad
\left\{\begin{array}{ll}\bar D^0 J/\psi & [\mathrm{IV}_F]\\ D^0 J/\psi & [\mathrm{IV}_D]\end{array}\right.,\\
B_s^0 \to &\left\{\begin{array}{ll}\bar D^0 \phi & [\mathrm{II}_S]\\ D^0 \phi & [\mathrm{II}_S]\end{array}\right., \quad
\left\{\begin{array}{ll}\bar D^0 K^0_{S,L} & [\mathrm{II}_F]\\ D^0 K^0_{S,L} & [\mathrm{II}_D]\end{array}\right., \quad
\left\{\begin{array}{ll}\bar D^0 J/\psi & [\mathrm{IV}_S]\\ D^0 J/\psi & [\mathrm{IV}_S]\end{array}\right..
\end{aligned}
\tag{88}
$$

In each example the lower decay depends on the weak phase $-\phi_{ub}$. The type-IV W-exchange graphs (Fig. 6) may well be highly suppressed compared to the type-II spectator graphs, although in view of the easy trigger for $J/\psi D$ these modes should be searched for. Among the eight candidates, $B_d^0 \to DK^0_{S,L}$ and $B_s^0 \to D\phi$ are the best in terms of size of the smaller branching ratio of the pair, which should be of order 10^{-5}. Since a very intricate time-dependent analysis is required to extract the full information from method 3, the B_s decays, for which the mixing parameter x_s is 26, are likely to be less useful than the B_d decays.

At a hadron collider where only all-charged daughters are used in reconstructing the B^0 about 1% of the D^0 decays will be useful. Accounting for dilutions due to mixing of the second B at a hadron collider, some 10^{10}-10^{11} B's are needed to implement method 3. At an e^+e^- collider, results of comparable statistical precision can likely be had with one order of magnitude less B's, but still a rather large number.

2.7 Method 4: Neutral B-Meson Decays to CP Eigenstates

The most well-known method for extracting CP-violating phases uses neutral B mesons that decay to CP-eigenstates f. In this case,

$$|\bar{f}\rangle \equiv CP|f\rangle = \eta|f\rangle \qquad \text{where} \qquad \eta = \begin{cases} +1 & CP(\text{even}) \\ -1 & CP(\text{odd}) \end{cases}. \tag{89}$$

The decay amplitude can be written,

$$A(B^0 \to f) = |A|\, e^{-i\phi_D} e^{i\delta}, \tag{90}$$

where δ is a strong-interaction phase, and the weak-interaction phase ϕ_D depends on whether the decay proceeds via a $\bar{b} \to \bar{c}$ or $\bar{u}$ transition,

$$\phi_D = \begin{cases} \phi_{cb} = 0, & b \to c \\ \phi_{ub}, & b \to u \end{cases}. \tag{91}$$

Following eq. (30) we can write the amplitude for the CP-conjugate process as

$$A(\bar{B}^0 \to \bar{f}) = \eta A(\bar{B}^0 \to f) = |A|\, e^{i\phi_D} e^{i\delta}, \quad \text{and hence} \quad A(\bar{B}^0 \to f) = \eta\, |A|\, e^{i\phi_D} e^{i\delta}, \tag{92}$$

using eq. (89). Combining eqs. (90-92) with (77), we arrive at the time-dependent decay rates

$$\begin{aligned} \Gamma(B^0(t) \to f) &\propto |A|^2\, e^{-t}[1 - \eta \sin(xt) \sin 2(\phi_M + \phi_D)], \\ \Gamma(\bar{B}^0(t) \to f) &\propto |A|^2\, e^{-t}[1 + \eta \sin(xt) \sin 2(\phi_M + \phi_D)]. \end{aligned} \tag{93}$$

If, as we have assumed, only a single graph contributes to $B^0 \to f$, then there is only a single strong-interaction phase δ in both this and the conjugate reaction $\bar{B}^0 \to f$. This single phase does not appear at all in the interference term in eq. (93).

Both ϕ_M and ϕ_D can take on two values depending on the decay considered, according to eqs. (78) and (91), so there are four classes of phase angles explored by method 4 as listed in Table 1. Classes 1, 2 and 3 provide measurements of ϕ_1, ϕ_2 and ϕ_3, respectively, of the unitarity test. Class-4 decays should show very little CP violation, but not necessarily zero, as they depend on V_{ts} which has a CP-violating phase at higher order (see eq. (21)). Any difference in the size of the CP violation between class 1 and class 2, or between class 3 and class 4 would indicate that the superweak model is not the source of that effect.

The class-1 decay $B_d^0 \to J/\psi K_S^0$ is particularly easy to trigger on and identify, and may provide the first evidence for CP violation in the B system. The most prominent class-2 and -3 decays, $B_d^0 \to \pi^+\pi^-$ and $B_s^0 \to \rho^0 K_S^0$, respectively, both have smaller branching ratios and in particular it may prove elusive to measure ϕ_3 with $B_s^0 \to \rho^0 K_S^0$.

Another potential difficulty is that with the exception of $B_d^0 \to J/\psi K_S^0$, all other decays to CP eigenstates have admixtures of penguin diagrams with different weak phases than the dominant tree diagram [76]. Hence, it is useful to have other procedures than method 4 to measure ϕ_2 and ϕ_3.

Table 1: The 23 basic neutral-B decays to CP eigenstates. The graphs associated with each decay mode are shown in fig. 6. The subscripts F, S, and D refer to CKM-favored (amplitude $\propto \lambda^2$), -suppressed ($\propto \lambda^3$), and -doubly-suppressed ($\propto \lambda^4$), respectively. The weak-interaction phase $\phi_M + \phi_D$ is shown in parentheses after each graph type, where ϕ_M is the phase due to mixing and ϕ_D is the phase due to $\bar{b}$-quark decay. Penguin graphs (V-VII) are included in classes 1-4 if they lead to the same final state as the nominal graphs for that class, even though their topology is different. Classes 1a and 4a are pure penguin graphs. Within each class the modes are ranked roughly in order of decreasing branching ratio. A final-state π^0 could be replaced by an η, ρ^0, ω, *etc.*, and a J/ψ could be replaced by an η_c, χ, ψ', *etc.*, but final states with two spin-1 particles must be analyzed according to method 6.

Class	B^0	$\bar{b} \to \overline{q}$	Modes	Graph($\phi_M + \phi_D$)
1	B_d^0	$\bar{b} \to \bar{c}$	$J/\psi K_{S,L}^0$	$\mathrm{II}_F(\phi_{td})$, $\mathrm{VI}_F(\phi_{td})$
			D^+D^-	$\mathrm{I}_S(\phi_{td})$, $\mathrm{IV}_S(\phi_{td})$, V_S, VII_S
			$J/\psi\pi^0$	$\mathrm{II}_S(\phi_{td})$, VI_S
			$D_s^+D_s^-$	$\mathrm{IV}_S(\phi_{td})$, V_S
			$\phi K_{S,L}^0$	$\mathrm{VI}_F(\phi_{td})$, $\mathrm{VII}_F(\phi_{td})$
2	B_d^0	$\bar{b} \to \bar{u}$	$\pi^+\pi^-$	$\mathrm{I}_S(\phi_{td}+\phi_{ub})$, $\mathrm{IV}_S(\phi_{td}+\phi_{ub})$, V_S, VII_S
			$\pi^0\pi^0$	$\mathrm{II}_S(\phi_{td}+\phi_{ub})$, $\mathrm{IV}_S(\phi_{td}+\phi_{ub})$, V_S, VI_S, VII_S
			$\rho^0 K_{S,L}^0$	$\mathrm{II}_D(\phi_{td}+\phi_{ub})$, $\mathrm{VI}_F(\phi_{td})$, $\mathrm{VII}_F(\phi_{td})$
			$D^0\bar{D}^0$	$\mathrm{IV}_S(\phi_{td}+\phi_{ub})$, V_S
			K^+K^-	$\mathrm{IV}_S(\phi_{td}+\phi_{ub})$, V_S
3	B_s^0	$\bar{b} \to \bar{u}$	$\rho^0 K_{S,L}^0$	$\mathrm{II}_S(\phi_{ub})$, $\mathrm{VI}_S(\phi_{td})$, $\mathrm{VII}_S(\phi_{td})$
			K^+K^-	$\mathrm{I}_D(\phi_{ub})$, $\mathrm{IV}_D(\phi_{ub})$, V_F, VII_F
			$\phi\pi^0$	$\mathrm{II}_D(\phi_{ub})$, VI_F
			$\pi^+\pi^-$	$\mathrm{IV}_D S(\phi_{ub})$, V_F,
			$\pi^0\pi^0$	$\mathrm{IV}_D S(\phi_{ub})$, V_F,
4	B_s^0	$\bar{b} \to \bar{c}$	$D_s^+D_s^-$	I_F, IV_F, V_F, VII_F
			$J/\psi K_{S,L}^0$	II_S, $\mathrm{VI}_S(\phi_{td})$
			$D^0\bar{D}^0$	IV_F, $\mathrm{IV}_D(\phi_{ub})$, V_F, V_S
			D^+D^-	IV_F, V_F
			$K^0\bar{K}^0$	V_F, VII_F
1a	B_s^0	$\bar{b} \to \bar{s}$	$\phi K_{S,L}^0$	$\mathrm{VI}_S(\phi_{td})$, $\mathrm{VII}_S(\phi_{td})$
4a	B_d^0	$\bar{b} \to \bar{u}$	$\phi\pi^0$	VI_S
			$K^0\bar{K}^0$	V_S, VII_S

2.8 Method 5: B Decays to Sets of Final States Related by Isospin

In Table 1 we see that the decay $B_d^0 \to \pi^+\pi^-$ that can be used to determine ϕ_2 has contributions both from spectator diagrams and penguin diagrams. However, the penguin diagrams have no weak phase [76] in this case, and to the extent that they are significant, the measurement of ϕ_2 is compromised.

By measurement of the related decays $B_u^+ \to \pi^+\pi^0$, $B_d^0 \to \pi^+\pi^-$, $\pi^0\pi^0$, the weak phase ϕ_2 can be isolated from the strong phase of the penguin diagram (which latter phase is not determined). The separation is aided by the fact that the spin-0 $\pi\pi$ final states can only be in isospin $I = 0$ or 2 states due to Bose statistics, and by the result that the penguin graphs can only lead to the $I = 0$ states [77].

The exchange-symmetric $\pi\pi$ isospin states of interest are,

$$\begin{aligned}
\sqrt{\tfrac{1}{2}}(|\pi^+\pi^0\rangle + |\pi^0\pi^+\rangle) &= |2,1\rangle, \\
\sqrt{\tfrac{1}{2}}(|\pi^+\pi^-\rangle + |\pi^-\pi^+\rangle) &= \sqrt{\tfrac{1}{3}}|2,0\rangle + \sqrt{\tfrac{2}{3}}|0,0\rangle, \\
|\pi^0\pi^0\rangle &= \sqrt{\tfrac{2}{3}}|2,0\rangle - \sqrt{\tfrac{1}{3}}|0,0\rangle, \\
\sqrt{\tfrac{1}{2}}(|\pi^-\pi^0\rangle + |\pi^0\pi^-\rangle) &= |2,-1\rangle,
\end{aligned} \tag{94}$$

via the relevant Clebsch-Gordon coefficients. The decays of a $B_d^0 = |\frac{1}{2}, -\frac{1}{2}\rangle$ or $B_u^+ = |\frac{1}{2}, \frac{1}{2}\rangle$ to these states involve $\Delta I_3 = \frac{1}{2}$ which can occur via either $\Delta I = \frac{1}{2}$ or $\frac{3}{2}$ transitions. We use the "spurion" notation to write the weak Hamiltonian for these transitions as,

$$H_{\rm weak} = \quad H_{1/2}|\tfrac{1}{2}, \tfrac{1}{2}\rangle + H_{3/2}|\tfrac{3}{2}, \tfrac{1}{2}\rangle. \tag{95}$$

Then the $\pi\pi$ isospin states obtained in the B decays are,

$$\begin{aligned}
H_{1/2}|\tfrac{1}{2}, \tfrac{1}{2}\rangle|B_d^0\rangle &= \sqrt{\tfrac{1}{2}}H_{1/2}|1,0\rangle + \sqrt{\tfrac{1}{2}}H_{1/2}|0,0\rangle, \\
H_{3/2}|\tfrac{3}{2}, \tfrac{1}{2}\rangle|B_d^0\rangle &= \sqrt{\tfrac{1}{2}}H_{3/2}|2,0\rangle + \sqrt{\tfrac{1}{2}}H_{3/2}|0,0\rangle, \\
H_{1/2}|\tfrac{1}{2}, \tfrac{1}{2}\rangle|B_u^+\rangle &= H_{1/2}|1,1\rangle, \\
H_{3/2}|\tfrac{3}{2}, \tfrac{1}{2}\rangle|B_u^+\rangle &= \sqrt{\tfrac{3}{4}}H_{3/2}|2,1\rangle - \sqrt{\tfrac{1}{4}}H_{3/2}|1,1\rangle.
\end{aligned} \tag{96}$$

The transition amplitudes are then,

$$\begin{aligned}
A(B_d^0 \to \pi^+\pi^-) \ &\equiv A^{+-} &&= \sqrt{\tfrac{1}{6}}\langle\pi\pi, I=2|H_{3/2}|B\rangle + \sqrt{\tfrac{1}{3}}\langle\pi\pi, I=0|H_{1/2}|B\rangle, \\
A(B_d^0 \to \pi^0\pi^0) \ &\equiv A^{00} &&= \sqrt{\tfrac{1}{3}}\langle\pi\pi, I=2|H_{3/2}|B\rangle - \sqrt{\tfrac{1}{6}}\langle\pi\pi, I=0|H_{1/2}|B\rangle, \\
A(B_u^+ \to \pi^+\pi^0) \ &\equiv A^{+0} &&= \sqrt{\tfrac{3}{4}}\langle\pi\pi, I=2|H_{3/2}|B\rangle.
\end{aligned} \tag{97}$$

Following [63], we define,

$$A_2 \equiv \quad \sqrt{\tfrac{1}{12}}\langle\pi\pi, I=2|H_{3/2}|B\rangle, \qquad \text{and} \qquad A_2 \equiv \ -\sqrt{\tfrac{1}{6}}\langle\pi\pi, I=0|H_{1/2}|B\rangle, \tag{98}$$

so we can write the three B-decay amplitudes (and the corresponding three $\bar{B}$ amplitudes) as,

$$\begin{aligned} A^{+0} &= 3A_2, & \bar{A}^{-0} &= 3\bar{A}_2, \\ A^{+-} &= \sqrt{2}(A_2 - A_0), & \bar{A}^{+-} &= \sqrt{2}(\bar{A}_2 - \bar{A}_0), \\ A^{00} &= 2A_2 + A_0, & \bar{A}^{00} &= 2\bar{A}_2 + \bar{A}_0. \end{aligned} \tag{99}$$

Thus the six decay amplitudes are related by the two constraints,

$$\sqrt{\tfrac{1}{2}}A^{+-} + A^{00} = A^{+0}, \qquad \sqrt{\tfrac{1}{2}}\bar{A}^{+-} + \bar{A}^{00} = \bar{A}^{-0}. \tag{100}$$

As isospin amplitudes A_2 and $\bar{A}_2$ contain only spectator graphs their phase structure can be written,

$$A_2 = |A_2|\, e^{i\phi_2} = |A_2|\, e^{-i\phi_{ub}} e^{i\delta_2}, \qquad \bar{A}_2 = |A_2|\, e^{i\overline{\phi}_2} = |A_2|\, e^{i\phi_{ub}} e^{i\delta_2}, \tag{101}$$

noting that the spectator graphs for A_2 involve a $\bar{b} \to \bar{u}$ transition, and defining δ_2 as the strong-interaction phase of the isospin-2 spectator graph. The amplitudes A_0 (later written $|A_0|\, e^{i\phi_0}$) and $\bar{A}_0$ ($= \left|\bar{A}_0\right| e^{i\overline{\phi}_0}$) contain both spectator and penguin graphs, but it will not be possible to separate these amplitudes in this analysis, so we do not write the equivalent of eq. (101) for them.

The decay rates are,

$$\begin{aligned} \Gamma(B^+ \to \pi^+\pi^0) &= \Gamma(B^- \to \pi^-\pi^0) \propto |A_2|^2, \\ \Gamma(B^0(t) \to \pi^+\pi^-) &\propto e^{-t}[K^{+-} - C^{+-}\cos(xt) - S^{+-}\sin(xt)], \\ \Gamma(\bar{B}^0(t) \to \pi^+\pi^-) &\propto e^{-t}[K^{+-} + C^{+-}\cos(xt) + S^{+-}\sin(xt)], \\ \Gamma(B^0(t) \to \pi^0\pi^0) &\propto e^{-t}[K^{00} - C^{00}\cos(xt) - S^{00}\sin(xt)], \\ \Gamma(\bar{B}^0(t) \to \pi^0\pi^0) &\propto e^{-t}[K^{00} + C^{00}\cos(xt) + S^{00}\sin(xt)], \end{aligned} \tag{102}$$

using eq. (77) and defining,

$$\begin{aligned} K^{+-} &= (\left|\bar{A}^{+-}\right|^2 + |A^{+-}|^2)/2, \\ C^{+-} &= (\left|\bar{A}^{+-}\right|^2 - |A^{+-}|^2)/2, \\ S^{+-} &= \mathrm{Im}(A^{*+-} e^{2i\phi_{td}} \bar{A}^{+-}) \\ &= 2\,|A_2|^2\, \mathrm{Im}\left[e^{2i(\phi_{td}+\phi_{ub})}\left(1 - \tfrac{|A_0|}{|A_2|} e^{i(\phi_2-\phi_0)}\right)\left(1 - \tfrac{\left|\bar{A}_0\right|}{|A_2|} e^{-i(\overline{\phi}_2-\overline{\phi}_0)}\right)\right], \\ K^{00} &= (\left|\bar{A}^{00}\right|^2 + |A^{00}|^2)/2, \\ C^{00} &= (\left|\bar{A}^{00}\right|^2 - |A^{00}|^2)/2, \\ S^{00} &= \mathrm{Im}(A^{*00} e^{2i\phi_{td}} \bar{A}^{00}) \\ &= 4\,|A_2|^2\, \mathrm{Im}\left[e^{2i(\phi_{td}+\phi_{ub})}\left(1 + \tfrac{1}{2}\tfrac{|A_0|}{|A_2|} e^{i(\phi_2-\phi_0)}\right)\left(1 + \tfrac{1}{2}\tfrac{\left|\bar{A}_0\right|}{|A_2|} e^{-i(\overline{\phi}_2-\overline{\phi}_0)}\right)\right], \end{aligned} \tag{103}$$

where we have used eqs. (99) in obtaining the second forms for the coefficients S.

Assuming the Fourier analysis of the time-dependent neutral B-decays rates (102) can be performed, the coefficients K and C determine the magnitudes $|A^{+-}|$, $|\bar{A}^{+-}|$, $|A^{00}|$ and $|\bar{A}^{00}|$. From $\Gamma(B^{\pm} \to \pi^{\pm}\pi^{0})$ we know $|A^{+0}| = |\bar{A}^{-0}| = |A_2|$. Thus, the magnitudes of all six quantities in the constraint equations (100) are known. Interpreting these constraints as triangles in the complex plane as shown in Fig. 5, we can calculate the phase differences $|\phi_2 - \phi^{+-}|$, $|\phi_2 - \phi^{00}|$, $\left|\overline{\phi}_2 - \overline{\phi}^{+-}\right|$ and $\left|\overline{\phi}_2 - \overline{\phi}^{00}\right|$ using the cosine law. Then, using the second (or third) of eqs. (99) we can calculate $|A_0|$, $|\phi_2 - \phi_0|$, $|\bar{A}_0|$ and $|\overline{\phi}_2 - \overline{\phi}_0|$.

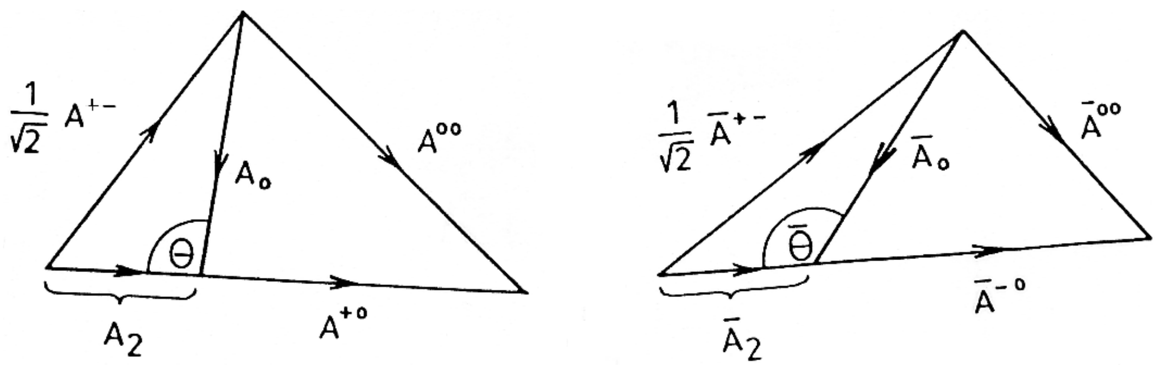

Figure 5: The isospin decomposition (99) of the$B \to \pi\pi$ decay amplitudes, and the constraint relations (100) are shown as triangles on the complex plane. An ambiguity remains as to the signs of the phase differences $\phi_2 - \phi_0$ and $\overline{\phi}_2 - \overline{\phi}_0$ as each triangle could be reflected about the A_2 or $\bar{A}_2$ axis.

Thus, we know the magnitudes of all quantities appearing in the expressions for S^{+-} and S^{00}, but there remains a fourfold ambiguity as to the phase, since only the absolute values of $\phi_2 - \phi_0$ and $\overline{\phi}_2 - \overline{\phi}_0$ have been determined. Therefore, we can obtain two sets of four solutions for $\sin 2(\phi_{td} + \phi_{ub}) = \sin 2\phi_2$. The true solution should be the only common value in both sets. In principle, this method removes the uncertainty in the measurement of ϕ_2 due to penguin graphs.

In practice, method 5 will be difficult to implement. The spectator graph for $B_d^0 \to \pi^0\pi^0$ is type-II, color-suppressed so the branching ratio may well be an order of magnitude smaller than that for $B_d^0 \to \pi^+\pi^-$. As method 5 depends heavily on reconstruction of B decays with final-state π^0's for which no secondary-vertex information will be available, it may be impossible to implement it at a hadron collider and it will be experimentally challenging at an e^+e^- collider. Searches for other final states than $\pi\pi$ for use with the isospin method have, however, not yielded any better candidate thus far [64, 65, 66].

2.9 Method 6: Angular Analysis of B Decays to Mixtures of CP Eigenstates

When applying method 4 to neutral B-mesons decays to CP eigenstates we cannot immediately use self-conjugate final states that consist of a pair of vector mesons (such as $D^{\star}\bar{D}^{\star}$), or of three or more mesons (such as $J/\psi K_S^0 \pi^0$). Depending on whether the orbital angular momentum is even or odd, the CP of the final state changes sign. If we know the fraction p of decays to the CP-even final state we can write eq. (93) as,

$$\begin{aligned} \Gamma(B^0(t) \to f) &\propto |A|^2 e^{-t}[1 + (1-2p)\sin(xt)\sin 2(\phi_M + \phi_D)], \\ \Gamma(\bar{B}^0(t) \to f) &\propto |A|^2 e^{-t}[1 - (1-2p)\sin(xt)\sin 2(\phi_M + \phi_D)], \end{aligned} \tag{104}$$

and a measurement of $\sin 2(\phi_M + \phi_D)$ can be made subject to the dilution factor $1 - 2p$. The fraction p can in general be determined by analysis of the angular distribution of the sequential decays of the final-state mesons, as discussed in detail in ref. [71] and references therein. Such an angular analysis will require sizable event samples, perhaps an order of magnitude larger than needed for method 4.

A simplified angular analysis will suffice if the final state consists of a vector meson plus two spinless mesons. When all three mesons are self conjugate (such as $J/\psi K_S^0 \pi^0$), helicity-zero decays have definite CP and their abundance determined from a single angular distribution [70]. When the spin-0 mesons come from the decay of a spin-1 meson, and the two spin-1 mesons are each self conjugate (such as $D^{\star 0}\rho^0$ or $J/\psi\phi$), or the two vector mesons are antiparticles (such as $D^{\star +}D^{\star -}$) the so-called transversity analysis can be used to extract p [71].

Referring to Table 1, we see that the most interesting candidates for angular analysis are the decays $B_d^0 \to J/\psi K_S^0 \pi^0$ and $D^{\star +}D^{\star -}$ from class 1, $B_d^0 \to \rho^+\rho^-$ and $\rho^0\rho^0$ from class 2, $B_s^0 \to \rho^0 K_S^0 \pi^0$ from class 3, and $B_s^0 \to D_s^{\star +}D_s^{\star -}$ and $J/\psi\phi$ from class 4. It is notable that most of these decays require photon detection.

A Appendix : Nonleptonic Decay Modes of the B Mesons

A survey of seven possible graphs describing B-meson decay indicates that the B_u will have 21 basic 2-body nonleptonic decays, the B_d will have 27, the B_s will have 29, and the B_c will have 21 (see Tables 2-5). This contrasts with the case for the K_u $(= K^+)$ and K_d $(= K^0)$ which each only have 2 such decays (not all distinct!). In the B system there are 24 basic decays to CP eigenstates compared to the 2 in the K system. All 98 of the basic two-body decays of the B-meson system have all-charged final states (at some price in secondary branching fraction), while only 1 of the basic K decays is all charged.

We have not displayed the catalog of decays of the B_c^+ $(= \bar{b}c)$, in which the charm quark decays before the b-quark, as is expected to happen in the majority of decays. Both the B_s and the B_c will be better studied at a hadron collider than at a low-energy e^+e^- collider.

The Tables refer to seven kinds of graphs, two spectator, annihilation, exchange, penguin/annihilation, and two penguin/spectator, as shown in Fig. 6. We can roughly estimate that for spectator graphs I:

CKM-favored decays have amplitudes $\propto \lambda^2$, and branching fractions of 10^{-2}-10^{-3};

CKM-suppressed decays have amplitudes $\propto \lambda^3$, and branching fractions of 3×10^{-4}-3×10^{-5};

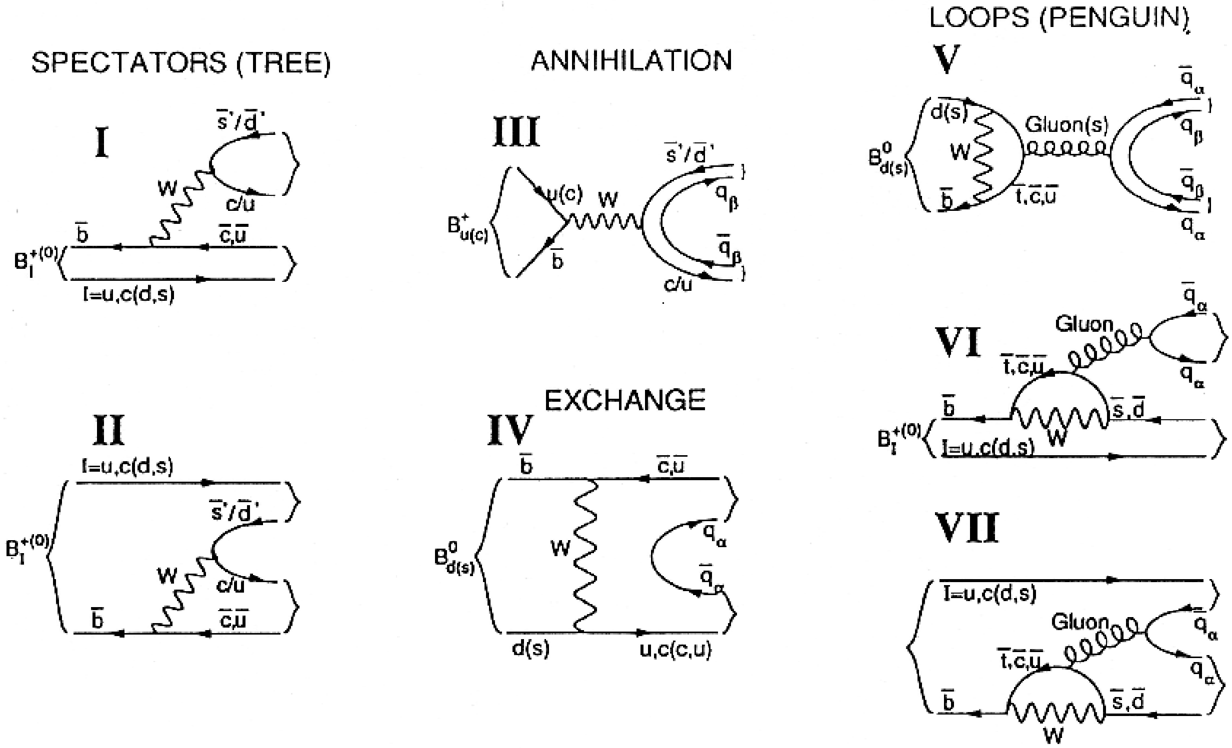

Figure 6: Seven graphs for the nonleptonic decays of B mesons.

CKM-doubly-suppressed decays have amplitudes $\propto \lambda^4$, and branching fractions of 10^{-5}-10^{-6}.

Graphs II, III and IV are 'color suppressed' in that only 1/3 of the quark pairs created by the W or gluons will have the proper color to match the other final-state quark pair, and so the rates are typically suppressed by a factor of 1/10 compared to graph I at the same order in λ.

The annihilation graph III and the exchange graph IV are controversial and both may be heavily suppressed.

Graphs V-VII are 'penguins,' which have yet to be observed in the laboratory. This suggests that they are suppressed by a factor of order 0.01 compared to graphs I and II at the same order in λ. Graphs V and VII are color-suppressed compared to graph VI. The weak phase of the amplitude for a penguin graph is ϕ_{td} if the transition is $\bar{b} \to \bar{d}$ (CKM-suppressed), and 1 for $\bar{b} \to \bar{s}$, as discussed by London and Peccei [76].

The two-body final states listed in the Tables are representative of the particular $q\bar{q}/q\bar{q}$ combination for each entry. All final states could be augmented by $n(\pi^+\pi^-)$, with possibly larger branching fractions. Likewise, every spin-0 final-state particle could be replaced by its spin-1 partner, and *vice versa.* Typically, the branch to the spin-1 meson will be 3 times that to the spin-0 partner.

The secondary decays used in constructing the last column of the Tables are:

Decay Mode . . . . Branching Ratio

$K_S^0 \to \pi^+\pi^-$	0.69
$\rho^0 \to \pi^+\pi^-$	1.00
$K^{\star 0} \to K^+\pi^-$	0.67
$\phi \to K^+K^-$	0.50
$D^+ \to K^-\pi^+\pi^+$	0.08
$D^0 \to K^-\pi^+$	0.04
$D_s^+ \to \phi\pi^+$	0.03
$D_s^+ \to \phi\pi^+\pi^+\pi^-$	0.04
$J/\psi \to e^+e^-$	0.07

For completeness will list the basic two-body nonleptonic decays of the D^+, D_s^+, and D^0 mesons in Tables 6-8.

Table 2: The 21 basic 2-body nonleptonic decays of the B_u^+ ($= \bar{b}u$). Figure 6 illustrates the seven types of graphs. The subscripts F, S, and D to the type of graph in this and following three tables refer to CKM-favored (ampli $\propto \lambda^2$), -suppressed (ampli $\propto \lambda^3$), and -doubly-suppressed (ampli $\propto \lambda^4$), respectively. If the decay amplitude depends on a CP-violating phase, the relevant phase of a CKM-matrix element is indicated in parentheses. The decay modes are listed roughly in order of decreasing branching fraction.

Graph	Final Quarks	Final State	All-Charged Daughters
I_F, II_F	$u\bar{c}/u\bar{d}$	$\bar{D}^0\pi^+$	$K^+\pi^-\pi^+$
I_F, $\mathrm{III}_D(\phi_{ub})$, VII_F	$c\bar{s}/u\bar{c}$	$D_s^+\bar{D}^0$	$K^+K^-\pi^+K^+\pi^-$
II_F, VI_F	$c\bar{c}/u\bar{s}$	$J/\psi K^+$	$e^+e^-K^+$
I_S	$c\bar{s}/u\bar{u}$	$D_s^+\rho^0$	$K^+K^-\pi^+\pi^+\pi^-$
I_S, II_S	$u\bar{c}/u\bar{s}$	$\bar{D}^0K^+$	$K^+\pi^-K^+$
I_S, $\mathrm{III}_S(\phi_{ub})$, $\mathrm{VII}_S(\phi_{td})$	$c\bar{d}/u\bar{c}$	$D^+\bar{D}^0$	$K^-\pi^+\pi^+K^+\pi^-$
$\mathrm{I}_S(\phi_{ub})$, $\mathrm{II}_S(\phi_{ub})$, $\mathrm{III}_S(\phi_{ub})$, VI_F, VII_F	$u\bar{u}/u\bar{d}$	$\rho^0\pi^+$	$\pi^+\pi^-\pi^+$
II_S, $\mathrm{VI}_S(\phi_{td})$	$c\bar{c}/u\bar{d}$	$J/\psi\pi^+$	$e^+e^-\pi^+$
$\mathrm{II}_S(\phi_{ub})$, $\mathrm{III}_S(\phi_{ub})$	$c\bar{u}/u\bar{s}$	D^0K^+	$K^-\pi^+K^+$
$\mathrm{I}_D(\phi_{ub})$, $\mathrm{II}_D(\phi_{ub})$, $\mathrm{III}_D(\phi_{ub})$, VI_F, VII_F	$u\bar{u}/u\bar{s}$	ρ^0K^+	$\pi^+\pi^-K^+$
$\mathrm{I}_D(\phi_{ub})$, $\mathrm{III}_D(\phi_{ub})$	$c\bar{d}/u\bar{u}$	$D^+\rho^0$	$K^-\pi^+\pi^+\pi^+\pi^-$
$\mathrm{II}_D(\phi_{ub})$, $\mathrm{III}_D(\phi_{ub})$	$c\bar{u}/u\bar{d}$	$D^0\pi^+$	$K^-\pi^+\pi^+$
$\mathrm{III}_S(\phi_{ub})$, $\mathrm{VII}_S(\phi_{td})$	$u\bar{s}/s\bar{d}$	$K^+\bar{K}^{\star 0}$	$K^+K^-\pi^+$
$\mathrm{III}_S(\phi_{ub})$	$c\bar{d}/d\bar{s}$	$D^+K^{\star 0}$	$K^-\pi^+\pi^+K^+\pi^-$
$\mathrm{III}_S(\phi_{ub})$	$c\bar{s}/s\bar{s}$	$D_s^+\phi$	$K^+K^-\pi^+K^+K^-$
$\mathrm{III}_S(\phi_{ub})$	$c\bar{c}/c\bar{s}$	$J/\psi D_s^+$	$e^+e^-K^+K^-\pi^+$
$\mathrm{III}_D(\phi_{ub})$, VII_F	$d\bar{s}/u\bar{d}$	$K^{\star 0}\pi^+$	$K^+\pi^-\pi^+$
$\mathrm{III}_D(\phi_{ub})$, VI_F, VII_F	$s\bar{s}/u\bar{s}$	ϕK^+	$K^+K^-K^+$
$\mathrm{III}_D(\phi_{ub})$	$c\bar{s}/s\bar{d}$	$D_s^+\bar{K}^{\star 0}$	$K^+K^-\pi^+K^-\pi^+$
$\mathrm{III}_D(\phi_{ub})$	$c\bar{c}/c\bar{d}$	$J/\psi D^+$	$e^+e^-K^-\pi^+\pi^+$
$\mathrm{VI}_S(\phi_{td})$	$s\bar{s}/u\bar{d}$	$\phi\pi^+$	$K^+K^-\pi^+$

Table 3: The 27 basic 2-body nonleptonic decays of the B_d^0 $(=\bar{b}d)$. The numbers in the "CP Eigenstate" column refer to the classification described in sec. 2.3.1 regarding the relevant CKM-phases governing the decay asymmetries. Graphs leading to CP-eigenstates includes a phase factor in ϕ_{td} due to mixing. However, in penguin graphs with $\bar{b} \to \bar{d}$ transitions to CP eigenstates, the two phase factors in ϕ_{td} cancel.

Graph	Final Quarks	Final State	CP Eigenstate	All-Charged Daughters
I_F, IV_F	$d\bar{c}/u\bar{d}$	$D^-\pi^+$		$K^+\pi^-\pi^-\pi^+$
I_F, VII_F	$c\bar{s}/d\bar{c}$	$D_s^+D^-$		$K^+K^-\pi^+K^+\pi^-\pi^-$
II_F, IV_F	$u\bar{c}/d\bar{d}$	$\bar{D}^0\rho^0$		$K^+\pi^-\pi^+\pi^-$
$\mathrm{II}_F(\phi_{td})$, $\mathrm{VI}_F(\phi_{td})$	$c\bar{c}/d\bar{s}$	$J/\psi K_S^0$	1	$e^+e^-\pi^+\pi^-$
I_S	$d\bar{c}/u\bar{s}$	D^-K^+		$K^+\pi^-\pi^-K^+$
$\mathrm{I}_S(\phi_{td})$, $\mathrm{IV}_S(\phi_{td})$, V_S, VII_S	$c\bar{d}/d\bar{c}$	D^+D^-	1, 4	$K^-\pi^+\pi^+K^+\pi^-\pi^-$
$\mathrm{I}_S(\phi_{td}+\phi_{ub})$, $\mathrm{IV}_S(\phi_{td}+\phi_{ub})$, V_S, VII_S	$u\bar{d}/d\bar{u}$	$\pi^+\pi^-$	2, 4	$\pi^+\pi^-$
$\mathrm{I}_S(\phi_{ub})$	$c\bar{s}/d\bar{u}$	$D_s^+\pi^-$		$K^+K^-\pi^+\pi^-$
II_S	$u\bar{c}/d\bar{s}$	$\bar{D}^0K^{\star 0}$		$K^+\pi^-K^+\pi^-$
$\mathrm{II}_S(\phi_{ub})$	$c\bar{u}/d\bar{s}$	$D^0K^{\star 0}$		$K^-\pi^+K^+\pi^-$
$\mathrm{II}_S(\phi_{td})$, VI_S	$c\bar{c}/d\bar{d}$	$J/\psi\rho^0$	1, 4	$e^+e^-\pi^+\pi^-$
$\mathrm{II}_S(\phi_{td}+\phi_{ub})$, $\mathrm{IV}_S(\phi_{td}+\phi_{ub})$, V_S, VI_S, VII_S	$u\bar{u}/d\bar{d}$	$\rho^0\rho^0$	2, 4	$\pi^+\pi^-\pi^+\pi^-$
$\mathrm{I}_D(\phi_{ub})$, VII_F	$u\bar{s}/d\bar{u}$	$K^+\pi^-$		$K^+\pi^-$
$\mathrm{I}_D(\phi_{ub})$, $\mathrm{IV}_D(\phi_{ub})$	$c\bar{d}/d\bar{u}$	$D^+\pi^-$		$K^-\pi^+\pi^+\pi^-$
$\mathrm{II}_D(\phi_{td}+\phi_{ub})$, $\mathrm{VI}_F(\phi_{td})$, $\mathrm{VII}_F(\phi_{td})$	$u\bar{u}/d\bar{s}$	$\rho^0K_S^0$	2, 1	$\pi^+\pi^-\pi^+\pi^-$
$\mathrm{II}_D(\phi_{ub})$, $\mathrm{IV}_D(\phi_{ub})$	$c\bar{u}/d\bar{d}$	$D^0\rho^0$		$K^-\pi^+\pi^+\pi^-$
IV_F	$s\bar{c}/u\bar{s}$	$D_s^-K^+$		$K^+K^-\pi^-K^+$
IV_F	$c\bar{c}/u\bar{c}$	$J/\psi\bar{D}^0$		$e^+e^-K^+\pi^-$
$\mathrm{IV}_S(\phi_{td}+\phi_{ub})$, V_S	$c\bar{u}/u\bar{c}$	$D^0\bar{D}^0$	2, 4	$K^-\pi^+K^+\pi^-$
$\mathrm{IV}_S(\phi_{td})$, V_S	$c\bar{s}/s\bar{c}$	$D_s^+D_s^-$	1, 4	$K^+K^-\pi^+K^+K^-\pi^-$
$\mathrm{IV}_S(\phi_{td}+\phi_{ub})$, V_S	$u\bar{s}/s\bar{u}$	K^+K^-	2, 4	K^+K^-
$\mathrm{IV}_D(\phi_{ub})$	$c\bar{s}/s\bar{u}$	$D_s^+K^-$		$K^+K^-\pi^+K^-$
$\mathrm{IV}_D(\phi_{ub})$	$c\bar{c}/c\bar{u}$	$J/\psi D^0$		$e^+e^-K^-\pi^+$
$\mathrm{VI}_F(\phi_{td})$, $\mathrm{VII}_F(\phi_{td})$	$s\bar{s}/d\bar{s}$	ϕK_S^0	1	$K^+K^-\pi^+\pi^-$
V_S	$s\bar{s}/s\bar{s}$	$\phi\phi$	4	$K^+K^-K^+K^-$
VI_S	$s\bar{s}/d\bar{d}$	$\phi\rho^0$	4	$K^+K^-\pi^+\pi^-$
V_S, VII_S	$s\bar{d}/d\bar{s}$	$\bar{K}^{\star 0}K^{\star 0}$	4	$K^-\pi^+K^+\pi^-$

Table 4: The 29 basic 2-body nonleptonic decays of the B_s^0 $(= \bar{b}s)$.

Graph	Final Quarks	Final State	CP Eigenstate	All-Charged Daughters
I_F	$s\bar{c}/u\bar{d}$	$D_s^- \pi^+$		$K^+K^-\pi^-\pi^+$
I_F, IV_F, V_F, VII_F	$c\bar{s}/s\bar{c}$	$D_s^+ D_s^-$	4	$K^+K^-\pi^+K^+K^-\pi^-$
II_F	$u\bar{c}/s\bar{d}$	$\bar{D}^0\bar{K}^{\star 0}$		$K^+\pi^-K^-\pi^+$
II_F, VI_F	$c\bar{c}/s\bar{s}$	$J/\psi\phi$	4	$e^+e^-K^+K^-$
I_S, IV_S	$s\bar{c}/u\bar{s}$	$D_s^- K^+$		$K^+K^-\pi^-K^+$
I_S, $\mathrm{VII}_S(\phi_{td})$	$s\bar{c}/c\bar{d}$	$D_s^- D^+$		$K^+K^-\pi^-K^-\pi^+\pi^+$
I_S, $\mathrm{VII}_S(\phi_{td})$	$s\bar{u}/u\bar{d}$	$K^-\pi^+$		$K^-\pi^+$
$\mathrm{I}_S(\phi_{ub})$, $\mathrm{IV}_S(\phi_{ub})$	$c\bar{s}/s\bar{u}$	$D_s^+ K^-$		$K^+K^-\pi^+K^-$
II_S	$u\bar{c}/s\bar{s}$	$\bar{D}^0\phi$		$K^+\pi^-K^+K^-$
$\mathrm{II}_S(\phi_{ub})$	$c\bar{u}/s\bar{s}$	$D^0\phi$		$K^-\pi^+K^+K^-$
II_S, $\mathrm{VI}_S(\phi_{td})$	$c\bar{c}/s\bar{d}$	$J/\psi K_S^0$	4, 1	$e^+e^-\pi^+\pi^-$
$\mathrm{II}_S(\phi_{ub})$, $\mathrm{VI}_S(\phi_{td})$, $\mathrm{VII}_S(\phi_{td})$	$u\bar{u}/s\bar{d}$	$\rho^0 K_S^0$	3, 1	$\pi^+\pi^-\pi^+\pi^-$
$\mathrm{I}_D(\phi_{ub})$, $\mathrm{IV}_D(\phi_{ub})$, V_F, VII_F	$u\bar{s}/s\bar{u}$	K^+K^-	3, 4	K^+K^-
$\mathrm{I}_D(\phi_{ub})$	$c\bar{d}/s\bar{u}$	D^+K^-		$K^-\pi^+\pi^+K^-$
$\mathrm{II}_D(\phi_{ub})$, VI_F	$s\bar{s}/u\bar{u}$	$\phi\rho^0$	3, 4	$K^+K^-\pi^+\pi^-$
$\mathrm{II}_D(\phi_{ub})$	$c\bar{u}/s\bar{d}$	$D^0\bar{K}^{\star 0}$		$K^-\pi^+K^-\pi^+$
IV_F, $\mathrm{IV}_D(\phi_{ub})$ V_F, V_S	$c\bar{u}/u\bar{c}$	$D^0\bar{D}^0$	4, 3	$K^-\pi^+K^+\pi^-$
IV_F, V_F	$c\bar{d}/d\bar{c}$	D^+D^-	4	$K^-\pi^+\pi^+K^+\pi^-\pi^-$
IV_S	$d\bar{c}/u\bar{d}$	$D^-\pi^+$		$K^+\pi^-\pi^-\pi^+$
IV_S	$u\bar{c}/u\bar{u}$	$\bar{D}^0\rho^0$		$K^+\pi^-\pi^+\pi^-$
IV_S	$c\bar{c}/u\bar{c}$	$J/\psi\bar{D}^0$		$e^+e^-K^+\pi^-$
$\mathrm{IV}_S(\phi_{ub})$	$c\bar{d}/d\bar{u}$	$D^+\pi^-$		$K^-\pi^+\pi^+\pi^-$
$\mathrm{IV}_S(\phi_{ub})$	$c\bar{u}/u\bar{u}$	$D^0\rho^0$		$K^-\pi^+\pi^+\pi^-$
$\mathrm{IV}_S(\phi_{ub})$	$c\bar{c}/c\bar{u}$	$J/\psi D^0$		$e^+e^-K^-\pi^+$
$\mathrm{IV}_D(\phi_{ub})$, V_F	$u\bar{d}/d\bar{u}$	$\pi^+\pi^-$	3, 4	$\pi^+\pi^-$
$\mathrm{IV}_D(\phi_{ub})$, V_F	$u\bar{u}/u\bar{u}$	$\rho^0\rho^0$	3, 4	$\pi^+\pi^-\pi^+\pi^-$
V_F, VII_F	$s\bar{s}/s\bar{s}$	$\phi\phi$	4	$K^+K^-K^+K^-$
V_F, VII_F	$d\bar{s}/s\bar{d}$	$K^{\star 0}\bar{K}^{\star 0}$	4	$K^+\pi^-K^-\pi^+-$
$\mathrm{VI}_S(\phi_{td})$, $\mathrm{VII}_S(\phi_{td})$	$s\bar{s}/s\bar{d}$	ϕK_S^0	1	$K^+K^-\pi^+\pi^-$

Table 5: The 21 basic 2-body nonleptonic decays of the B_c^+ $(= \bar{b}c)$ in which the $\bar{b}$-quark decays before the c-quark.

Graph	Final Quarks	Final State	All-Charged Daughters
I_F	$c\bar{c}/u\bar{d}$	$J/\psi\pi^+$	$e^+e^-\pi^+$
I_F, II_F, III_F, VI_F, VII_F	$c\bar{c}/c\bar{s}$	$J/\psi D_s^+$	$e^+e^-K^+K^-\pi^+$
II_F, III_F	$c\bar{d}/u\bar{c}$	$D^+\bar{D}^0$	$K^-\pi^+\pi^+K^+\pi^-$
I_S	$c\bar{c}/u\bar{s}$	$J/\psi K^+$	$e^+e^-K^+$
I_S, II_S, III_S, $\mathrm{VI}_S(\phi_{td})$, $\mathrm{VII}_S(\phi_{td})$	$c\bar{c}/c\bar{d}$	$J/\psi D^+$	$e^+e^-K^-\pi^+\pi^+$
$\mathrm{I}_S(\phi_{ub})$, III_S, $\mathrm{VII}_S(\phi_{td})$	$c\bar{u}/u\bar{d}$	$D^0\pi^+$	$K^-\pi^+\pi^+$
$\mathrm{I}_S(\phi_{ub})$, $\mathrm{II}_S(\phi_{ub})$	$c\bar{s}/c\bar{u}$	$D_s^+D^0$	$K^+K^-\pi^+K^-\pi^+$
II_S, III_S	$c\bar{s}/u\bar{c}$	$D_s^+\bar{D}^0$	$K^+\pi^-K^+K^-\pi^+$
$\mathrm{II}_S(\phi_{ub})$, III_S, $\mathrm{VI}_S(\phi_{td})$, $\mathrm{VII}_S(\phi_{td})$	$c\bar{d}/u\bar{u}$	$D^+\rho^0$	$\pi^+\pi^-K^-\pi^+\pi^+$
$\mathrm{I}_D(\phi_{ub})$, III_F, VII_F	$c\bar{u}/u\bar{s}$	D^0K^+	$K^-\pi^+K^+$
$\mathrm{I}_D(\phi_{ub})$, $\mathrm{II}_D(\phi_{ub})$	$c\bar{d}/c\bar{u}$	D^+D^0	$K^-\pi^+\pi^+K^-\pi^+$
$\mathrm{II}_D(\phi_{ub})$, VI_F	$c\bar{s}/u\bar{u}$	$D_s^+\rho^0$	$K^+K^-\pi^+\pi^+\pi^-$
III_F	$u\bar{u}/u\bar{d}$	$\rho^0\pi^+$	$\pi^+\pi^-\pi^+$
III_F	$u\bar{s}/s\bar{d}$	$K^+K_S^0$	$K^+\pi^+\pi^-$
III_F, VII_F	$c\bar{d}/d\bar{s}$	$D^+K_S^0$	$K^-\pi^+\pi^+\pi^+\pi^-$
III_F, VI_F, VII_F	$c\bar{s}/s\bar{s}$	$D_s^+\phi$	$K^+K^-\pi^+K^+K^-$
III_S	$u\bar{u}/u\bar{s}$	ρ^0K^+	$\pi^+\pi^-K^+$
III_S	$d\bar{s}/u\bar{d}$	$K_S^0\pi^+$	$\pi^+\pi^-\pi^+$
III_S	$s\bar{s}/u\bar{s}$	ϕK^+	$K^+K^-K^+$
III_S, $\mathrm{VII}_S(\phi_{td})$	$c\bar{s}/s\bar{d}$	$D_s^+K_S^0$	$K^+K^-\pi^+\pi^+\pi^-$
$\mathrm{VI}_S(\phi_{td})$	$c\bar{d}/s\bar{s}$	$D^+\phi$	$K^-\pi^+\pi^+K^+K^-$

Table 6: The 7 basic 2-body nonleptonic decays of the D^+ $(= c\bar{d})$. In this and the following two tables penguin contributions are ignored.

Graph	Final Quarks	Final State	All-Charged Daughters
I_F, II_F	$s\bar{d}/u\bar{d}$	$\bar{K}^{\star 0}\pi^+$	$K^-\pi^+\pi^+$
I_S, III_S	$s\bar{d}/u\bar{s}$	$\bar{K}^{\star 0}K^+$	$K^-\pi^+K^+$
I_S, II_S, III_S	$d\bar{d}/u\bar{d}$	$\rho^0\pi^+$	$\pi^+\pi^-\pi^+$
II_S	$s\bar{s}/u\bar{d}$	$\phi\pi^+$	$K^+K^-\pi^+$
I_D, III_D	$d\bar{d}/u\bar{s}$	ρ^0K^+	$\pi^+\pi^-K^+$
II_D, III_D	$d\bar{s}/u\bar{d}$	$K^{\star 0}\pi^+$	$K^+\pi^-\pi^+$
III_D	$s\bar{s}/u\bar{s}$	ϕK^+	$K^+K^-K^+$

Table 7: The 6 basic 2-body nonleptonic decays of the D_s^+ ($= c\bar{s}$).

Graph	Final Quarks	Final State	All-Charged Daughters
I_F	$s\bar{s}/u\bar{d}$	$\phi\pi^+$	$K^+K^-\pi^+$
II_F, III_F	$s\bar{d}/u\bar{s}$	$\bar{K}^{\star 0}K^+$	$K^-\pi^+K^+$
I_S, II_S, III_S	$s\bar{s}/u\bar{s}$	ϕK^+	$K^+K^-K^+$
I_S, III_S	$d\bar{s}/u\bar{d}$	$K^{\star 0}\pi^+$	$K^+\pi^-\pi^+$
II_S, III_S	$d\bar{d}/u\bar{s}$	ρ^0K^+	$\pi^+\pi^-K^+$
III_F	$u\bar{u}/u\bar{d}$	$\rho^0\pi^+$	$\pi^+\pi^-\pi^+$

Table 8: The 11 basic 2-body nonleptonic decays of the D^0 ($= c\bar{u}$).

Graph	Final Quarks	Final State	All-Charged Daughters
I_F, IV_F	$s\bar{u}/u\bar{d}$	$K^-\pi^+$	$K^-\pi^+$
II_F	$s\bar{s}/u\bar{u}$	$\phi\rho^0$	$K^+K^-\pi^+\pi^-$
I_S, IV_S	$u\bar{d}/d\bar{u}$	$\pi^+\pi^-$	$\pi^+\pi^-$
I_S, IV_S	$u\bar{s}/s\bar{u}$	K^+K^-	K^+K^-
II_S, IV_S	$s\bar{d}/u\bar{u}$	$\bar{K}^{\star 0}\rho^0$	$K^-\pi^+\pi^+\pi^-$
II_S, IV_S	$d\bar{s}/u\bar{u}$	$K^{\star 0}\rho^0$	$K^+\pi^-\pi^+\pi^-$
II_S, IV_S	$d\bar{u}/u\bar{d}$	$\rho^0\rho^0$	$\pi^+\pi^-\pi^+\pi^-$
I_D, IV_D	$u\bar{s}/d\bar{u}$	$K^+\pi^-$	$K^+\pi^-$
IV_F	$s\bar{s}/s\bar{d}$	$\phi\bar{K}^{\star 0}$	$K^+K^-K^-\pi^+$
IV_S	$d\bar{s}/s\bar{d}$	$K^{\star 0}\bar{K}^{\star 0}$	$K^+\pi^-K^-\pi^+$
IV_D	$s\bar{s}/d\bar{s}$	$\phi K^{\star 0}$	$K^+K^-K^+\pi^-$

B Appendix: Maximum-Likelihood Analysis of CP-Violating Asymmetries

As an illustration of some of the methods used in data analysis of experiments on CP violation in the B-meson system, we deduce estimates of the statistical precision of analyses of CP-violating asymmetries in the B^0-$\bar{B}^0$ system via the maximum-likelihood method. In the case of B^0 decays to a CP eigenstate f the decay-time distributions have the form (45),

$$N_\pm(t) = \frac{N}{2} e^{-t}(1 \pm A \sin xt),$$

where N is the total number of decays to state f, A is the CP-violating parameter which is a simple function of parameters of the CKM-matrix, $x = \Delta M/\Gamma$ is the mixing parameter, and $+(-)$ labels decays in which the B was born as a $B^0(\bar{B}^0)$. The estimated error on the measurement of A can be written in terms of dilution factors D as

$$\sigma_A = \frac{1}{D\sqrt{N}},$$

where

$$D = \frac{x}{1+x^2}$$

for a time-integrated analysis;

$$D = D_t \sqrt{\frac{2x^2}{1+4x^2}}$$

for a time-dependent analysis;

$$D = D_t \frac{x}{1+x^2}\sqrt{\frac{1+2x^4}{1+4x^2}}$$

for an analysis based only on the shape of the decay distribution; and

$$D_t = e^{-x^2\sigma_t^2/2}$$

represents the effect of time resolution σ_t. Results are also presented for simultaneous analysis of the CP-violating parameter A and the mixing parameter x, and for analysis of the mixing parameter via decays to non-CP eigenstates. We end with an analysis of asymmetries appropriate for study of CP violation at an e^+e^- collider.

B.1 Introduction

An optimum analysis of CP-violating asymmetries will be based on the maximum-likelihood method. This should yield greater statistical precision than the methods presented in, say, [78] and [79]. Here, we deduce the size of the error on various asymmetries via the likelihood technique.

The principal example we consider is the case of neutral-B-meson decay to a CP eigenstate f (called method 4 above). Here we suppose that we have a sample of N decays of either a B^0 or $\bar{B}^0$ to state f in an experiment where there are equal numbers of B and $\bar{B}$'s produced. Then, following eq. (26) of [79] the time distribution of the observed decays can be written,

$$N_{\pm}(t) = \frac{N}{2} e^{-t}(1 \pm A \sin xt), \tag{105}$$

where throughout this Appendix time is measured in units of the B^0 lifetime, and A is a simple function of the parameters of the CKM-matrix (in the Standard Model). The subscript $+$ means that the decay occurred for a B that was a B^0 at $t = 0$, while subscript $-$ means the B was a $\bar{B}^0$ at $t = 0$. These initial conditions must be determined by observation of the second B in the event. For hadroproduction of B's the effect of tagging the second B factorizes from the analysis of the first and we do not consider the second B in this note (except in sec. B.11 on e^+e^- colliders).

When A is nonzero there is CP violation, which manifests itself both in the difference between the shape of distributions $N_+(t)$ and $N_-(t)$, and in the difference between the total number of decays of each type:

$$N_{\pm} \equiv \int_0^{\infty} N_{\pm}(t) dt = \frac{N}{2}\left(1 \pm A \frac{x}{1+x^2}\right). \tag{106}$$

Eventually we will wish to consider the effect of the experimental resolution in time t on the analysis. It is felicitous that this has only a minor effect on the formalism, so we prepare the general case now. We designate σ_t as the r.m.s. time resolution, which means that the observed decays distributions can be obtained by convolution [80]:

$$\begin{aligned} N_{\pm}(t) &= \frac{N}{2}\int_{-\infty}^{\infty} \frac{e^{-(t-t')^2/2\sigma_t^2}}{\sqrt{2\pi}\sigma_t} dt' e^{-t'}(1 \pm A \sin xt') \\ &= \frac{N}{2} e^{\sigma_t^2/2} e^{-t}\left(1 \pm A e^{-x^2\sigma_t^2/2} \sin x(t - \sigma_t^2)\right) \\ &\approx \frac{N}{2} e^{-t}(1 \pm A e^{-x^2\sigma_t^2/2} \sin xt), \end{aligned} \tag{107}$$

using integral 3.896.4 of ref. [81], and where the approximation holds well when $\sigma_t \ll 1$ (*i.e.*, when the time resolution is much better than a lifetime), as is expected to be the case when a silicon vertex detector is used.

Hence an analysis of distributions of the form,

$$N_{\pm}(t) = \frac{N}{2} e^{-t}(1 \pm a \sin xt) \tag{108}$$

includes the effect of time resolution if we write,

$$a = AD_t, \qquad \text{with} \qquad D_t \equiv e^{-x^2\sigma_t^2/2} \tag{109}$$

where D_t is the "dilution factor" associated with finite time resolution.

We anticipate that an analysis of B^0-$\bar{B}^0$ mixing will be similar to that of CP violation. In the case of mixing, we take $N_+(t)$ to be the distribution of decays in which the B was born as a B^0 and decayed as a B^0 (or was born as a $\bar{B}^0$ and decayed as a $\bar{B}^0$), while $N_-(t)$

is the distribution of decays in which the B was born as a B^0 and decayed as a $\bar{B}^0$ (or was born as a $\bar{B}^0$ and decayed as a B^0. For this, we must be able to tell whether the particle was a B^0 or $\bar{B}^0$ at the time of decay, and so we cannot use the CP-eigenstates discussed above – unless there is CP violation, for which case the statistical precision will typically be greatly reduced, as discussed later.

The mixing time distributions have the form (recalling eq. (18)),

$$N_{\pm}(t) = N\,|F_{\pm}(t)|^2 = \frac{N}{2} e^{-t}(1 \pm \cos xt), \tag{110}$$

leading to integrated numbers of events,

$$N_{\pm} = \frac{N}{2}\int_0^{\infty} e^{-t}(1 \pm \cos xt) = \frac{N}{2}\left(1 \pm \frac{1}{1+x^2}\right). \tag{111}$$

As before, the effect of a time resolution σ_t is readily included via convolution with a Gaussian,

$$\begin{aligned} N_{\pm}(t) &= \frac{N}{2}\int_{-\infty}^{\infty} \frac{e^{-(t-t')^2/2\sigma_t^2}}{\sqrt{2\pi}\sigma_t} dt' e^{-t'}(1 \pm \cos xt') \\ &= \frac{N}{2} e^{\sigma_t^2/2} e^{-t}\left(1 \pm e^{-x^2\sigma_t^2/2}\cos x(t-\sigma_t^2)\right) \\ &\approx \frac{N}{2} e^{-t}(1 \pm e^{-x^2\sigma_t^2/2}\cos xt), \end{aligned} \tag{112}$$

Hence, a general mixing analysis will deal with distributions of form,

$$N_{\pm}(t) = \frac{N}{2} e^{-t}(1 \pm a\cos xt), \tag{113}$$

which are closely related to those for CP violation given in eq. (108).

B.2 The Maximum-Likelihood Method

We recall the technique of data analysis via maximizing the likelihood by the example of N data points x_i sampled from a Gaussian distribution of mean a and variance σ,

$$P(x,a) = \frac{e^{-(x-a)^2/2\sigma^2}}{\sqrt{2\pi}\sigma}. \tag{114}$$

The probability (or likelihood) of observing the data set $\{x_i\}$ is then,

$$\mathcal{L}(a) = \prod_{i=1}^{N} P(x_i, a). \tag{115}$$

The idea of the maximum-likelihood method [82] is that $\mathcal{L}$ is approximately Gaussian in the parameter a (whether or not $P(x,a)$ is a Gaussian function of x), and hence the value of a

that maximizes $\mathcal{L}(a)$ is the best estimate of a. Further, an excellent estimate of the error on the measurement of a follows from the second derivative of $\ln \mathcal{L}$,

$$\begin{aligned}
\mathcal{L} &= \prod_{i=1}^{N} e^{-(x_i-a)^2/2\sigma^2}, && (116)\\
\ln \mathcal{L} &= -\frac{1}{2}\sum_{i=1}^{N}\frac{(x_i-a)^2}{\sigma^2}, && (117)\\
\frac{d\ln \mathcal{L}}{da} &= \frac{1}{2}\sum_i \frac{x_i-a}{\sigma^2}, && (118)\\
\frac{d^2\ln \mathcal{L}}{da^2} &= -\sum_i \frac{1}{\sigma^2} = -\frac{N}{\sigma^2}. && (119)
\end{aligned}$$

The maximum of $\mathcal{L}$ and for $\ln \mathcal{L}$ occur at the same value of a, namely $a = \sum_i x_i/N$ as expected. We identify,

$$-\frac{d^2\ln \mathcal{L}}{da^2} \equiv \frac{1}{\sigma_a^2} \tag{120}$$

to find that $\sigma_a = \sigma/\sqrt{N}$ as expected.

The method is readily extended to distributions that depend on multiple parameters. We will later consider two parameters, say a and b, for which the likelihood function $\mathcal{L}(a, b)$ formed from products of the probabilities $P(x_i, a, b)$ is expected to be Gaussian in a and b,

$$\mathcal{L}(a,b) \propto \exp\left\{-\frac{1}{2}\left(\frac{(a-a_{\rm true})^2}{\sigma_a^2} + \frac{2(a-a_{\rm true})(b-b_{\rm true})}{\sigma_{ab}^2} + \frac{(b-b_{\rm true})^2}{2\sigma_b^2}\right)\right\}. \tag{121}$$

Hence, our estimates on the errors of the fitted values of a and b will be,

$$\frac{1}{\sigma_a^2} = -\frac{\partial^2\ln \mathcal{L}}{\partial a^2}, \qquad \frac{1}{\sigma_{ab}^2} = -\frac{\partial^2\ln \mathcal{L}}{\partial a\partial b}, \qquad \frac{1}{\sigma_b^2} = -\frac{\partial^2\ln \mathcal{L}}{\partial b^2}. \tag{122}$$

B.3 Analysis of a Simple Asymmetry

As a preliminary example of the maximum-likelihood method, we consider the case when the data can take on only two values, labeled + and −, with probability,

$$P_\pm = \frac{1 \pm a}{2}, \tag{123}$$

where a is the asymmetry parameter. For an experiment in which N_+ and N_- events are observed, we form the likelihood function,

$$\mathcal{L} = \left(\frac{1+a}{2}\right)^{N_+}\left(\frac{1-a}{2}\right)^{N_-}. \tag{124}$$

The needed derivatives of $\ln \mathcal{L}$ are,

$$\begin{aligned} \ln \mathcal{L} &= N_+ \ln(1+a) + N_- \ln(1-a) + \text{constant}, & (125) \\ \frac{d \ln \mathcal{L}}{da} &= \frac{N_+}{1+a} - \frac{N_-}{1-a}, & (126) \\ \frac{d^2 \ln \mathcal{L}}{da^2} &= -\frac{N_+}{(1+a)^2} - \frac{N_-}{(1-a)^2}. & (127) \end{aligned}$$

On setting the first derivative to zero, we find the usual expression for the asymmetry,

$$a = \frac{N_+ - N_-}{N_+ + N_-}. \tag{128}$$

From this we express N_+ and N_- in terms of a and $N = N_+ + N_-$ to evaluate the error on the estimate of a as,

$$\sigma_a = \sqrt{\frac{1-a^2}{N}}, \tag{129}$$

using eq. (120). This agrees with the usual analysis based on the binomial distribution.

B.4 Time-Integrated Analysis of CP Violation

After these lengthy preliminaries, we turn to the analysis of CP-violating asymmetries, beginning with the case where the data in integrated over time to yield the total numbers of events given in eq. (106). In this case we study a simple asymmetry related by,

$$a = A\frac{x}{1+x^2} = AD_{t-\text{int}}, \tag{130}$$

where A is the CP-violating factor introduced in eq. (105), and we define,

$$D_{t-\text{int}} \equiv \frac{x}{1+x^2} \tag{131}$$

as the dilution factor due to time integration.

From eq. (129) we estimate the error on the measurement of A as,

$$\sigma_A = \frac{\sigma_a}{D_{t-\text{int}}} = \frac{1}{D_{t-\text{int}}}\sqrt{\frac{1-A^2D_{t-\text{int}}^2}{N}} \approx \frac{1}{D_{t-\text{int}}\sqrt{N}} = \frac{1+x^2}{x\sqrt{N}}, \tag{132}$$

where the approximation holds for small values of $AD_{t-\text{int}}$.

The error on A is large for both large and small values of the mixing parameter x. The minimum error as a function of x occurs if $x = 1$, for which $\sigma_A = 2/\sqrt{N}$. As $x \approx 1/\sqrt{2}$ for the B_d^0-meson, a time-integrated analysis is rather effective in this case.

B.5 Time-Dependent Analysis of CP Violation

We now determine what additional statistical power can be expected if we perform an analysis of the time-dependent CP-violating decay distributions given in eq. (105). The likelihood function is then,

$$\mathcal{L} = \prod_i e^{-t_i}(1 + A\sin xt_i) \prod_j e^{-t_j}(1 - A\sin xt_j), \tag{133}$$

where subscript i labels events in which the B was born as a B^0, and j labels events in which the B was born as a $\bar{B}^0$. This form of the likelihood function is normalized to include information both on the shape as well as the integral of the decay distributions.

According to eq. (120) we estimate the error on the measurement of A as,

$$\frac{1}{\sigma_A^2} = -\frac{d^2 \ln \mathcal{L}}{dA^2} = \sum_i \frac{\sin^2 xt_i}{(1 + A\sin xt_i)^2} + \sum_j \frac{\sin^2 xt_j}{(1 - A\sin xt_j)^2}. \tag{134}$$

We estimate the sums by integrals according to,

$$\sum_{i(j)} f(t) \approx \frac{N}{2} \int_0^\infty dt e^{-t}(1 \pm A\sin xt) f(t), \tag{135}$$

which leads to

$$\frac{1}{\sigma_A^2} = N \int_0^\infty \frac{dt e^{-t} \sin^2 xt}{1 - A^2 \sin^2 xt} \approx N \int_0^\infty dt e^{-t} \sin^2 xt = \frac{2x^2 N}{1 + 4x^2}, \tag{136}$$

where we ignore the time-varying term in the denominator for small A, and we have used integral 3.895.1 of [81].

The full integral can be expressed as an infinite series on expanding the denominator in a Taylor series. Keeping the first correction we find that,

$$\frac{1}{\sigma_A^2} \approx N \int_0^\infty dt e^{-t} \sin^2 xt (1 + A^2 \sin^2 xt) = \frac{2x^2 N}{1 + 4x^2} \left(1 + \frac{12A^2 x^2}{1 + 16x^2}\right). \tag{137}$$

Thus even for $A = \frac{1}{3}$ the correction is at most 8% for any value of x.

We summarize the result (136) by writing,

$$\sigma_A \approx \frac{1}{D_{t-\mathrm{dep}}\sqrt{N}} \qquad \text{with} \qquad D_{t-\mathrm{dep}} \equiv \sqrt{\frac{2x^2}{1 + 4x^2}}. \tag{138}$$

The time-dependent dilution factor $D_{t-\mathrm{dep}}$ is larger than the time integrated factor (from eq. (131)) for any value of x, and consequently the time-dependent analysis is always more powerful statistically, as is to be expected.

In particular, the time-dependent analysis remains very powerful for large x, where a time-integrated analysis yields no information. Indeed, for the time-dependent analysis,

$$\sigma_A \approx \sqrt{\frac{2}{N}} \qquad \text{for large } x. \tag{139}$$

This result also compares favorably with that reported in [78] and [79], where it was argued that the effective dilution factor at large x is the average of $\sin xt$ over a half-cycle, namely $2/\pi$, leading to $\sigma_A \approx \pi/2\sqrt{N}$.

B.6 Analysis of the Shape of the Time Distribution

M. Purohit has noted [83] that one could also perform an analysis of CP violation based only on the shape of the decay distributions, ignoring the CP-violating asymmetry in the integrated decay rates. Such an analysis would be the only one possible if the experiment consisted of B's born only as B^0 (or only as $\bar{B}^0$).

The analysis is based on a likelihood function in which the decay distribution is normalized to one (using the notation of eq. (133) and assuming equal numbers of B^0 and $\bar{B}^0$ initially),

$$\mathcal{L} = \prod_i \frac{e^{-t_i}(1 + A\sin xt_i)}{1 + A\frac{x}{1+x^2}} \prod_j \frac{e^{-t_j}(1 - A\sin xt_j)}{1 - A\frac{x}{1+x^2}}. \tag{140}$$

Approximating the sums in the second derivative of $\ln \mathcal{L}$ by the appropriate integrals, and again neglecting a factor in A^2 in the denominator, we have,

$$\sigma_A \approx \frac{1}{D_{\rm shape}\sqrt{N}} \qquad \text{with} \qquad D_{\rm shape} \equiv \frac{x}{1+x^2}\sqrt{\frac{1+2x^4}{1+4x^2}}. \tag{141}$$

This result is, of course, poorer than the full time-dependent analysis (eq. (138)), but approaches the same accuracy for large x where only the shape matters. The shape analysis is less powerful than the time-integrated analysis (eq. (132)) for $x < \sqrt{2}$, which includes the case of B_d^0-mesons.

The full time-dependent analysis of the previous section can be considered as the proper combination of the time-integrated and the shape analyses. We readily verify the validity of this by noting that,

$$\frac{1}{\sigma^2(\text{time-dependent})} = \frac{1}{\sigma^2(\text{time-integrated})} + \frac{1}{\sigma^2(\text{shape})}, \tag{142}$$

on comparing eqs. (132), (138), and (141).

As a numerical example, we consider the case of $x = 1/\sqrt{2}$, as holds approximately for B_d^0-mesons. We then have,

$$\sigma(\text{time-dependent}) = \sqrt{\frac{3}{N}} = \frac{1.73}{\sqrt{N}}, \qquad \sigma(\text{time-integrated}) = \frac{3}{\sqrt{2N}} = \frac{2.12}{\sqrt{N}},$$
$$\sigma(\text{shape}) = \frac{3}{\sqrt{N}}. \tag{143}$$

It is remarkable that the time-dependent analysis is only 20% better than the time-integrated analysis, while the former requires a costly silicon vertex detector.

B.7 The Effect of Time Resolution

In sec. B.1 we noted that the effect on the analysis of a time resolution σ_t is well approximated by a dilution factor $D_t = e^{-x^2\sigma_t^2/2}$ multiplying the CP-violating parameter A (see eqs. 107)-(109)). Thus, the full-time-dependent analysis including time resolution will yield,

$$\sigma_A \approx \frac{1}{D_{t-{\rm dep}}D_t\sqrt{N}} = \sqrt{\frac{1+4x^2}{2x^2}}\frac{e^{x^2\sigma_t^2/2}}{\sqrt{N}}. \tag{144}$$

The effect of time resolution is only noticeable for $xt \gtrsim 1$, *i.e.*, for large x, in which case,

$$\sigma_A \approx e^{x^2\sigma_t^2/2}\sqrt{\frac{2}{N}} \qquad \text{(large } x\text{)}. \tag{145}$$

B.8 The Effect of a Cut at Short Times

M. Purohit has also pointed out [83] that in a realistic analysis based on decay times reconstructed with a silicon vertex detector there will be a loss of events for times t less than some small time t_0, when the secondary vertex cannot be distinguished from the primary. In this case the full time-dependent analysis proceeds as in sec. B.5, except that when estimating sums by integrals we now use,

$$\sum_{i(j)} f(t) \approx \frac{N}{2}\int_{t_0}^{\infty} dte^{-t}(1 \pm A\sin xt)f(t), \tag{146}$$

which leads to,

$$\frac{1}{\sigma_A^2} \approx N\int_{t_0}^{\infty} dte^{-t}\sin^2 xt = \frac{e^{-t_0}N}{2}\left(1 + \frac{2x\sin 2xt_0 - \cos 2xt_0}{1+4x^2}\right), \tag{147}$$

using integral 2.663.1 of ref. [81]. As $c\tau \approx 320$ μm is the B-decay length, and the typical resolution of silicon vertex detector is less than 20 μm, the condition $t_0 \ll 1$ lifetime will likely be satisfied. Then, for small x we can write,

$$\frac{1}{\sigma_A^2} \approx \frac{2x^2N}{1+4x^2}\left(1 - \frac{t_0^3}{6}(1+4x^2)\right), \qquad (x \ll 1), \tag{148}$$

which implies a very small correction. For large x we have,

$$\frac{1}{\sigma_A^2} \approx \frac{N}{2}(1-t_0), \qquad (x \gg 1), \tag{149}$$

which indicates that the correction for the cut at small times is small but perhaps notable in this case.

B.9 Simultaneous Analysis of Parameters A and x

In all of the proceeding we have tacitly assumed that the value of the mixing parameter x is known from other studies. This might not be so for B_s^0 mesons (at the time of the writing (1992) of this Appendix).

Here we consider the time-dependent likelihood function (133) to estimate the errors on measurement of both A and x according to the procedure of eq. (122). The effect of time resolution is included as the dilution factor D_t to parameter A. With the same approximation of sums as integrals we find,

$$\frac{1}{\sigma_A^2} \approx \frac{2x^2e^{-x^2\sigma_t^2}N}{1+4x^2}, \qquad \frac{1}{\sigma_{Ax}^2} \approx Ae^{-x^2\sigma_t^2}N\int_0^{\infty} dte^{-t}t\sin xt\cos xt = \frac{Ae^{-x^2\sigma_t^2}N\sin(2\tan^{-1}2x)}{2(1+4x^2)},$$
$$\frac{1}{\sigma_x^2} \approx A^2e^{-x^2\sigma_t^2}\int_0^{\infty} dte^{-t}t^2\cos^2 xt = A^2e^{-x^2\sigma_t^2}N\left(1 + \frac{\cos(3\tan^{-1}2x)}{(1+4x^2)^{3/2}}\right) \tag{150}$$

using integrals 3.944.5 and 3.944.6 of [81].

These complicated results are perhaps best illustrated by considering the limits of small and large x. For small x,

$$\frac{1}{\sigma_A^2} \approx 2x^2 N, \qquad \frac{1}{\sigma_{Ax}^2} \approx 2AxN, \qquad \frac{1}{\sigma_x^2} \approx 2A^2 N, \qquad \text{(small } x\text{)}. \tag{151}$$

The result for σ_x suggests that surprisingly good resolution in x can be obtained even when the mixing oscillations are almost indiscernible. However, one must note the correlation of the errors in x and A. More properly, we should report the error in x as the extreme value of the 1-σ error ellipse (from eq. (121)),

$$\frac{A^2}{\sigma_A^2} + \frac{2Ax}{\sigma_{Ax}^2} + \frac{x^2}{\sigma_x^2} = 1. \tag{152}$$

On requiring $dx/dA = 0$ in this, we find that the extreme value satisfies $x = A\sigma_{Ax}^2/\sigma_A^2$. Inserting this into eq. (150) we must evaluate to sixth order to find,

$$\sigma_x(\text{effective}) \approx \frac{1}{Ax^2\sqrt{112N}}. \tag{153}$$

So indeed for small x it is very difficult to determine x from studies of CP violation.

For large x eq. (150) becomes,

$$\sigma_A \approx e^{x^2\sigma_t^2/2}\sqrt{\frac{2}{N}}, \qquad \sigma_{Ax} \to \infty, \qquad \sigma_x \approx \frac{e^{x^2\sigma_t^2/2}}{A\sqrt{N}}, \qquad \text{(large } x\text{)}. \tag{154}$$

As $x\sigma_t \to 1$, which may well hold for the B_s^0-meson, the resolution in both A and x deteriorate rapidly. It will be advantageous to have determined x in a separate measurement.

B.10 Analysis of B^0-$\bar{B}^0$ Mixing

As it will be advantageous to deduce the mixing parameter x for the B_s^0-meson from other than CP-violation data, we consider now the statistical power of such an analysis. This is based on eq. (110), or eq. (113) when time resolution is included. We form the likelihood function,

$$\mathcal{L} = \prod_i e^{-t_i}(1 + a\cos xt_i)\prod_j e^{-t_j}(1 - a\cos xt_j), \tag{155}$$

where $a = e^{-x^2\sigma_t^2/2}$ is the effect of time resolution, and subscript $i(j)$ refers to events where the B is born as a B^0 and decays as a $B^0(\bar{B}^0)$ (or where the B is born as a $\bar{B}^0$ and decays as a $\bar{B}^0(B^0)$).

Again approximating sums as integrals in the second derivative of $\ln\mathcal{L}$, we find that,

$$\frac{1}{\sigma_x^2} = N\int_0^\infty dt e^{-t}t^2 = 2N, \tag{156}$$

so that,

$$\sigma_x = \frac{1}{\sqrt{2N}} \tag{157}$$

if $xt \ll 1$ so that time resolution may be ignored.

When time resolution is significant we find,

$$\frac{1}{\sigma_x^2} = N e^{-x^2\sigma_t^2} \int_0^\infty \frac{dt e^{-t} t^2 \sin^2 xt}{1 - e^{-x^2\sigma_t^2}\cos^2 xt}. \tag{158}$$

This integral can be bounded by either considering the denominator to be 1 or $\sin^2 xt$, leading to,

$$e^{-x^2\sigma_t^2} N \left(1 - \frac{\cos(3\tan^{-1} 3x)}{(1+4x^2)^{3/2}}\right) \approx e^{-x^2\sigma_t^2} N \leq \frac{1}{\sigma_x^2} \leq 2e^{-x^2\sigma_t^2} N, \tag{159}$$

using integral 3.944.6 of ref. [81], and the approximation holds for large x. This implies,

$$\frac{e^{x^2\sigma_t^2/2}}{\sqrt{2N}} \leq \sigma_x \leq \frac{e^{x^2\sigma_t^2/2}}{\sqrt{N}} \tag{160}$$

holds for any x and σ_t. Furthermore, when one is not restricted to the use of decay modes leading to CP eigenstates the total number of events N may be much larger than in (154).

The effect of a cut at a small time t_0 is readily considered, as in sec. B.8. For small x the correction is fifth order in t_0, while for large x it is third order. That is, the correction is unimportant.

B.11 Analysis of CP Violation at an e^+e^- Collider

As discussed in sec. 2.3.4, when B's are produced are part of a B^0-$\bar{B}^0$ pair with definite charge conjugation, the analysis of CP violation is more intricate. In particular, if the B's are produced in a C-odd state, as from $\Upsilon(4S)$ decay, then a time-integrated asymmetry vanishes. However, good statistical power can be recovered by an analysis of time-resolved decay distributions.

Both B's of a B-$\bar{B}$ pair must be observed in the CP analysis.[17] We label B_1 as the (neutral) B that decays to the CP-eigenstate f, and B_2 as the (charged or neutral) B that decays to a state $g \neq \bar{g}$ that permits us to determine whether B_2 was a particle or antiparticle at the moment of its decay. We can accumulate four time distributions, where one B decays at time t_a and the other at time t_b with $t_a < t_b$,

$$\begin{aligned} I: &\quad \Gamma_{B_1\to f}(t_b)\Gamma_{B_2\to g}(t_a), \\ II: &\quad \Gamma_{B_1\to f}(t_a)\Gamma_{B_2\to g}(t_b), \\ III: &\quad \Gamma_{B_1\to f}(t_b)\Gamma_{\bar{B}_2\to \bar{g}}(t_a), \\ IV: &\quad \Gamma_{B_1\to f}(t_a)\Gamma_{\bar{B}_2\to \bar{g}}(t_b). \end{aligned} \tag{161}$$

[17]If the B's were produced at a symmetric e^+e^- collider, particularly at the $\Upsilon(4S)$ resonance where the rate is high, the latter is produced at rest and both B's would decay so close to their common production point that they could not be separately identified. This difficulty is avoided by use of an asymmetric e^+e^- collider (suggested by Oddone [75]) in which the center of mass of the e^+e^- collision is moving in the lab frame, such that in general the B^0 and $\bar{B}^0$ decay at locations sufficiently far apart that the two mesons can be distinguished.

The four distributions can be combined to form asymmetries in various ways: most relevant for C-odd states is,

$$A_1(t_a, t_b) \equiv \frac{II + III - I - IV}{I + II + III + IV}, \tag{162}$$

For C-even states we should consider,

$$A_2(t_a, t_b) \equiv \frac{III + IV - I - II}{I + II + III + IV}. \tag{163}$$

The third variation of such asymmetries turns out to vanish and is not considered further,

$$A_3(t_a, t_b) \equiv \frac{I + III - II - IV}{I + II + III + IV}. \tag{164}$$

For the case that mesons 1 and 2 are of the same type the four time distributions take the form,

$$\begin{aligned}
\Gamma_I(t_a, t_b) &\propto e^{-(t_a+t_b)}[1 \pm A \sin x(t_a \pm t_b)], \\
\Gamma_{II}(t_a, t_b) &\propto e^{-(t_a+t_b)}[1 + A \sin x(t_a \pm t_b)], \\
\Gamma_{III}(t_a, t_b) &\propto e^{-(t_a+t_b)}[1 \mp A \sin x(t_a \pm t_b)], \\
\Gamma_{IV}(t_a, t_b) &\propto e^{-(t_a+t_b)}[1 - A \sin x(t_a \pm t_b)],
\end{aligned} \tag{165}$$

where A the CP-violating factor introduced in eq. (105), and the lower sign in the distributions holds for C-odd states $|B_1\rangle|\bar{B}_2\rangle - |\bar{B}_1\rangle|B_2\rangle$.

Inserting the time distributions into the forms for the asymmetries we have,

$$\begin{aligned}
A_1 &= \begin{cases} A \sin x(t_a - t_b), & C(\text{odd}), \\ 0, & C(\text{even}), \end{cases} \\
A_2 &= \begin{cases} 0, & C(\text{odd}), \\ A \sin x(t_a + t_b), & C(\text{even}), \end{cases} \\
A_3 &= 0.
\end{aligned} \tag{166}$$

Clearly the asymmetry A_1 will be useful at an e^+e^- collider where only C-odd states are produced.

We first present a time-integrated analysis of these asymmetries, as discussed in [78]. Because of the time ordering in the definition of the distributions I-IV, the form of the integrals is,

$$\begin{aligned}
\int_0^\infty dt_a \int_{t_a}^\infty dt_b \Gamma_I(t_a, t_b) &= \frac{1}{2}\left(1 \pm A\frac{x}{1+x^2}\right), \qquad C(\text{odd}), \\
&= \frac{1}{2}\left(1 \pm A\frac{2x}{(1+x^2)^2}\right), \qquad C(\text{even}).
\end{aligned} \tag{167}$$

Thus we can write

$$A_1 = D_{1,t-\mathrm{int}} A \qquad \text{with} \qquad D_{1,t-\mathrm{int}} = \frac{x}{1+x^2} \qquad C(\text{odd}), \tag{168}$$

$$A_2 = D_{2,t-\mathrm{int}} A \qquad \text{with} \qquad D_{2,t-\mathrm{int}} = \frac{2x}{(1+x^2)^2} \qquad C(\text{even}). \tag{169}$$

The above results can be improved upon with a maximum-likelihood analysis. We label events in distributions I, II, III, and IV by indices i, j, k, and l, respectively, to form the likelihood function,

$$\mathcal{L} = \prod_i \Gamma_I(t_{ai}, t_{bi}) \prod_j \Gamma_{II}(t_{aj}, t_{bj}) \prod_k \Gamma_{III}(t_{ak}, t_{bk}) \prod_l \Gamma_{IV}(t_{al}, t_{bl}). \tag{170}$$

We again approximate the sums in the second derivative of $\ln \mathcal{L}$ via, sums as

$$\sum_i f(t_{ai}, t_{bi}) \to \frac{N}{2} \int_0^\infty dt_a \int_{t_a}^\infty dt_b \Gamma_I(t_a, t_b) f(t_a, t_b), \qquad \textit{etc.}, \tag{171}$$

for a total sample of N events, noting eq. (167). Ignoring the term in the denominator in A^2 the integrals are similar to those encountered previously,

$$\frac{1}{\sigma_A^2} \approx 2N \int_0^\infty dt_a e^{-t_a} \int_{t_a}^\infty dt_b e^{-t_b} \sin^2 x(t_a \pm t_b) = 2N \int_0^\infty dt_a e^{-2t_a} \int_0^\infty ds e^{-s} \sin^2 x(s + t_a \pm t_a), \tag{172}$$

where $s = t_a - t_b$. We characterize the results of the time-dependent analysis via the dilution factors,

$$D_{1,t-\mathrm{dep}} = \sqrt{\frac{2x^2}{1+4x^2}}, \quad C(\text{odd}), \qquad \text{and} \qquad D_{2,t-\mathrm{dep}} = \frac{\sqrt{8x^4+6x^2}}{1+4x^2}, \quad C(\text{even}). \tag{173}$$

The dilution factors from the time-dependent maximum-likelihood analysis are larger than those for the time-integrated analysis, and are the best possible. For large x, the time-dependent analysis is particularly advantageous.

As was mentioned in sec. B.5, the dilution factors for the case of large asymmetry A can be expressed as infinite series, the first terms of which are given in eq. (173). These series have been given in notes by Frank Porter [84].

The effect of time resolution σ_t on the analysis can be calculated as in eq. (107), and can be characterized (for small A) by the dilution factor,

$$D_t = e^{-x^2\sigma_t^2} \qquad \text{in the relation} \qquad \sigma_{A_{1,2}} = \frac{1}{D_{1,2} D_t \sqrt{N}}. \tag{174}$$

As both B's must be time-resolved in this analysis, the dilution factor D_t is the square of that encountered in the single-B analysis. Viewed another way, since two times are measured for each event at an e^+e^- collider the error on the sum or difference is $\sqrt{2}\sigma_t$. Using this in eq. (109) we also arrive at eq. (174).

References

[1] C.S. Wu *et al.*, *Experimental Test of Parity Conservation in Beta Decay*, Phys. Rev. **105**, 1413 (1957), http://kirkmcd.princeton.edu/examples/EP/wu_pr_105_1413_57.pdf

[2] L. Landau, *On the Conservation Laws for Weak Interactions*, Nucl. Phys. **3**, 127 (1957), http://kirkmcd.princeton.edu/examples/EP/landau_np_3_127_57.pdf

[3] T.D. Lee and C.N. Yang, *Parity Nonconservation and a Two-Component Theory of the Neutrino*, Phys. Rev. **105**, 1671 (1957), http://kirkmcd.princeton.edu/examples/EP/lee_pr_105_1671_57.pdf

[4] J.H. Christenson, J.W. Cronin, V.L. Fitch and R. Turlay, *Evidence for the* 2π *Decay of the* K_2^0 *Meson*, Phys. Rev. Lett. **13**, 138 (1964), http://kirkmcd.princeton.edu/examples/EP/christenson_prl_13_138_64.pdf

[5] J.W. Cronin, *The discovery of CP violation*, Eur. Phys. J. H **36**, 487 (2011), http://kirkmcd.princeton.edu/examples/EP/cronin_epjh_36_487_11.pdf

[6] R.G. Sachs, CP *Violation in* K^0 *Decays*, Phys. Rev. Lett. **13**, 286 (1964), http://kirkmcd.princeton.edu/examples/EP/sachs_prl_13_286_64.pdf

[7] L. Wolfenstein, *Violation of* CP *Invariance and the Possibility of Very Weak Interactions*, Phys. Rev. Lett. **13**, 562 (1964), http://kirkmcd.princeton.edu/examples/EP/wolfenstein_prl_13_562_64.pdf

[8] L. Wolfenstein, *The Superweak Theory 35 Years Later*, (June 14, 1999), http://kirkmcd.princeton.edu/examples/EP/wolfenstein_99.pdf

[9] B. Aubert *et al.*, *Observation of* CP *Violation in the* B^0 *Meson System*, Phys. Rev. Lett. **87**, 091801 (2001), http://kirkmcd.princeton.edu/examples/EP/aubert_prl_87_091801_01.pdf

[10] K. Aubert *et al.*, *Observation of Large* CP *Violation in the Neutral* B *Meson System*, Phys. Rev. Lett. **87**, 091802 (2001), http://kirkmcd.princeton.edu/examples/EP/abe_prl_87_091802_01.pdf

[11] J. Ellis, M.K. Gaillard, and D.V. Nanopoulos, *Left-Handed Currents and* CP *Violation*, Nucl. Phys. **B109**, 213 (1976), http://kirkmcd.princeton.edu/examples/EP/ellis_np_b109_213_76.pdf

[12] M.K. Gaillard, and B.W. Lee, *Rare decay modes of the* K *mesons in gauge theories*, Phys. Rev. D **10**, 897 (1974), http://kirkmcd.princeton.edu/examples/EP/gaillard_prd_10_897_74.pdf

[13] T.D. Lee and C.S. Wu, *Decays of Neutral* K *Mesons*, Ann. Rev. Nucl. Sci. **16**, 511 (1966), http://kirkmcd.princeton.edu/examples/EP/lee_arns_16_511_66.pdf

[14] R.H. Good *et al.*, *Regeneration of Neutral* K *Mesons and Their Mass Difference*, Phys. Rev. **124**, 1223 (1961), http://kirkmcd.princeton.edu/examples/EP/good_pr_124_1223_61.pdf

[15] V.L. Fitch, P.A. Piroué and R.B. Perkins, *Mass Difference of Neutral K Mesons*, Nuovo Cim. **22**, 1160 (1961), http://kirkmcd.princeton.edu/examples/EP/fitch_nc_22_1160_61.pdf

[16] G.W. Meisner, B.B. Crawford and F.S. Crawford, Jr, *Sign of the K_1^0-K_2^0 Mass Difference*, Phys. Rev. Lett. **17**, 492 (1966), http://kirkmcd.princeton.edu/examples/EP/meisner_prl_17_492_66.pdf

[17] J. Canter *et al.*, *Sign of the K_L^0-K_S^0 Mass Difference*, Phys. Rev. Lett. **17**, 942 (1966), http://kirkmcd.princeton.edu/examples/EP/canter_prl_17_942_66.pdf

[18] J.V. Jovanovitch *et al.*, *Experiment on the Sign and Magnitude of the K_L^0-K_S^0 Mass Difference*, Phys. Rev. Lett. **17**, 1075 (1966), http://kirkmcd.princeton.edu/examples/EP/jovanovich_prl_1075_66.pdf

[19] J.R. Batley *et al.*, *A precision measurement of direct CP violation in the decay of neutral kaons into two pions*, Phys. Lett. **B544**, 87 (2002), http://kirkmcd.princeton.edu/examples/EP/batley_Pl_b544_87_02.pdf

[20] E. Abouzaid *et al.*, *Precise measurements of direct CP violation, CPT symmetry, and other parameters in the neutral kaon system*, Phys. Rev. D **83**, 092001 (2011), http://kirkmcd.princeton.edu/examples/EP/abouzaid_prd_83_092001_11.pdf

[21] E. Fernandez *et al.*, *Lifetime of Particles Containing b Quarks*, Phys. Rev. Lett. **51**, 1022 (1983), http://kirkmcd.princeton.edu/examples/EP/fernandez_prl_51_1022_83.pdf

[22] N.S. Lockyer *et al.*, *Measurement of the Lifetime of Bottom Hadrons*, Phys. Rev. Lett. **51**, 1316 (1983), http://kirkmcd.princeton.edu/examples/EP/lockyer_prl_51_1316_83.pdf

[23] P.D. Acton *et al.*, *Measurement of the B_s^0 lifetime*, Phys. Lett. **B312**, 501 (1993), http://kirkmcd.princeton.edu/examples/EP/acton_Pl_b312_501_93.pdf

[24] J. Ellis *et al.*, *The Phenomenology of the Next Left-Handed Quarks*, Nucl. Phys. **B1131**, 285 (1977), http://kirkmcd.princeton.edu/examples/EP/ellis_np_b131_285_77.pdf

[25] J.S. Hagelin, *Weak Mass Mixing, CP Violation, and the Decay of b-Quark Mesons*, Phys. Rev. D **20**, 2893 (1979), http://kirkmcd.princeton.edu/examples/EP/hagelin_prd_20_2893_79.pdf

[26] C. Albajar *et al.*, *Search for B^0-$\bar{B}^0$ Oscillations at the CERN Proton-Antiproton Collider*, Phys. Lett. **186B**, 247 (1987), http://kirkmcd.princeton.edu/examples/EP/albajar_Pl_b186_247_87.pdf

[27] H. Albrecht *et al.*, *Observation of B^0-$\bar{B}^0$ Mixing*, Phys. Lett. **192B**, 245 (1987), http://kirkmcd.princeton.edu/examples/EP/albrecht_Pl_192b_245_87.pdf

[28] V.M. Abazov *et al.*, *Direct Limits on the B_s^0 Oscillation Frequency*, Phys. Rev. Lett. **97**, 021802 (2006), http://kirkmcd.princeton.edu/examples/EP/abazov_prl_97_021802_06.pdf

[29] A. Abulencia *et al.*, *Measurement of the B_s^0-$\bar{B}_s^0$ Oscillation Frequency*, Phys. Rev. Lett. **97**, 062003 (2006), http://kirkmcd.princeton.edu/examples/EP/abulencia_prl_97_062003_06.pdf

[30] B. Aubert *et al.*, *Evidence for D^0-$\bar{D}^0$ Mixing*, Phys. Rev. Lett. **98**, 211802 (2007), http://kirkmcd.princeton.edu/examples/EP/aubert_prl_98_211802_07.pdf

[31] M. Starič *et al.*, *Evidence for D^0-$\bar{D}^0$ Mixing*, Phys. Rev. Lett. **98**, 211803 (2007), http://kirkmcd.princeton.edu/examples/EP/staric_prl_98_211803_07.pdf

[32] R. Aaij *et al.*, *Precision measurement of the B_s^0-$\bar{B}_s^0$ oscillation frequency with the decay $B_s^0 \to D_s^- \pi^+$*, New J. Phys. **15**, 053021 (2013), http://kirkmcd.princeton.edu/examples/EP/aaij_njp_15_053021_13.pdf

[33] N. Cabbibo, *Unitary Symmetry and Leptonic Decays*, Phys. Rev. Lett. **10**, 531 (1963), http://kirkmcd.princeton.edu/examples/EP/cabibbo_prl_10_531_63.pdf

[34] M. Kobayashi and T. Maskawa, *CP-Violation in the Renormalizable Theory of Weak Interaction*, Prog. Theor. Phys. **49**, 652 (1973), http://kirkmcd.princeton.edu/examples/EP/kobayashi_ptp_49_652_73.pdf

[35] L. Miani, *CP Violation in Purely Lefthanded Weak Interactions*, Phys. Lett. **62B**, 183 (1976), http://kirkmcd.princeton.edu/examples/EP/miani_pl_62b_183_76.pdf

[36] L.-L. Chau and W.-Y. Keung, *Comments on the Parameterization of the Kobayashi-Maskawa Matrix*, Phys. Rev. Lett. **53**, 1802 (1984), http://kirkmcd.princeton.edu/examples/EP/chau_prl_53_1802_84.pdf

[37] Z. Maki, M. Nakagawa and S. Sakata, *Remarks on the Unified Model of Elementary Particles*, Prog. Theor. Phys. **28**, 879 (1962), http://kirkmcd.princeton.edu/examples/neutrinos/maki_ptp_28_870_62.pdf

[38] L. Wolfenstein, *Parameterization of the Kobayashi-Maskawa Matrix*, Phys. Rev. Lett. **51**, 1945 (1983), http://kirkmcd.princeton.edu/examples/EP/wolfenstein_prl_51_1945_83.pdf

[39] P. Krawczyk *et al.*, *Predictions of the CKM Model for CP Asymmetries in B Decay*, Nucl. Phys. **B307**, 19 (1988), http://kirkmcd.princeton.edu/examples/EP/krawczyk_np_b307_19_88.pdf

[40] C. Jarlskog, *Commutator of the Quark Mass Matrices in the Standard Electroweak Model and a Measure of Maximal CP Nonconservation*, Phys. Rev. Lett. **55**, 1039 (1985), http://kirkmcd.princeton.edu/examples/EP/jarlskog_prl_55_1039_85.pdf
A Basis Independent Formulation of the Connection Between Quark Mass Matrices, CP Violation and Experiment, Z. Phys. C **29**, 491 (1985), http://kirkmcd.princeton.edu/examples/EP/jarlskog_zp_c29_491_85.pdf

[41] J.D. Bjorken, *B Physics at D0*, handwritten notes dated June 26, 1987.

[42] J.D. Bjorken, *Determination of phases of generalized Kobayashi-Maskawa matrix elements from their magnitudes*, Phys. Rev. D **39**, 1396 (1989), http://kirkmcd.princeton.edu/examples/EP/bjorken_prd_39_1396_89.pdf

[43] C. Jarlskog and R. Stora, *Unitarity Polygons and CP Violation Areas and Phases in the Standard Electroweak Model*, Phys. Lett. **208B**, 268 (1988), http://kirkmcd.princeton.edu/examples/EP/jarlskog_pl_208b_268_88.pdf

[44] T.T. Wu and C.N. Yang, *Phenomenological Analysis of Violation of CP Invariance in Decays of K^0 and $\bar{K}^0$*, Phys. Rev. Lett. **13**, 380 (1964),
http://kirkmcd.princeton.edu/examples/EP/wu_prl_13_380_64.pdf

[45] C.O. Dib *et al.*, *Standard-model predictions for CP violation in B^0-meson decay*, Phys. Rev. D **41**, 1522 (1990), http://kirkmcd.princeton.edu/examples/EP/dib_prd_41_1522_90.pdf

[46] B. Aubert *et al.*, *Measurement of the branching fraction, polarization, and CP asymmetries in $B^0 \to \rho^0\rho^0$ decay, and implications for the CKM angle α*, Phys. Rev. D **78**, 071104 (2008), http://kirkmcd.princeton.edu/examples/EP/aubert_prd_78_071104_08.pdf

[47] A. Poluektov *et al.*, *Evidence for direct CP violation in the decay $B^\pm \to D^{(*)}K^\pm$, $D \to K_S^0\pi^+\pi^-$ and measurement of the CKM phase ϕ_3*, Phys. Rev. D **81**, 112002 (2010), http://kirkmcd.princeton.edu/examples/EP/poluektov_prd_81_112002_10.pdf

[48] P. del Amo Sanchez *et al.*, *Evidence for direct CP violation in the Measurement of the Cabbibo-Kobayashi-Maskawa Angle γ with $B^\mp \to D^{(*)}K^{(*)\mp}$ Decays*, Phys. Rev. Lett. **105**, 121801 (2010), http://kirkmcd.princeton.edu/examples/EP/delamosanchez_prl_105_121801_10.pdf

[49] A.B. Carter and A.I. Sanda, *CP Nonconservation in Cascade Decays of B Mesons*, Phys. Rev. Lett. **45**, 952 (1980),
http://kirkmcd.princeton.edu/examples/EP/carter_prl_45_952_80.pdf

[50] A.B. Carter and A.I. Sanda, *CP Violation in B-Meson Decays*, Phys. Rev. D **23**, 1567 (1981), http://kirkmcd.princeton.edu/examples/EP/carter_prd_23_1567_81.pdf

[51] M. Gronau and D. London, *How to Determine All the Angles of the Unitarity Triangle from $B_d^0 \to DK_S$ and $B_s^0 \to D\phi$*, Phys. Lett. **B253**, 483 (1991),
http://kirkmcd.princeton.edu/examples/EP/gronau_pl_253b_483_91.pdf

[52] M. Gronau and D. Wyler, *On Determining a Weak Phase from Charged B Decay Asymmetries*, Phys. Lett. **B265**, 172 (1991),
http://kirkmcd.princeton.edu/examples/EP/gronau_pl_b265_172_91.pdf

[53] I. Dunietz, *CP violation with Self-Tagging B_d Modes*, Phys. Lett. **B270**, 75 (1991),
http://kirkmcd.princeton.edu/examples/EP/dunietz_pl_b270_75_91.pdf

[54] D. Atwood, I. Dunietz and A. Soni, *Enhanced CP Violation with $B \to KD^0(\bar{D}^0)$ Modes and Extraction of the Cabibbo-Kobayashi-Maskawa Angle γ*, Phys. Rev. Lett. **78**, 3257 (1997), http://kirkmcd.princeton.edu/examples/EP/atwood_prl_78_3257_97.pdf

[55] A. Giri *et al.*, *Determining γ using $B^\pm \to DK^\pm$ with multibody D decays*, Phys. Rev. D **68**, 054018 (2003), http://kirkmcd.princeton.edu/examples/EP/giri_prd_68_054018_03.pdf

[56] R. Aleksan *et al.*, *Determining the CP-Violating Phase γ*, Z. Phys. C **54**, 653 (1992),
http://kirkmcd.princeton.edu/examples/EP/aleksan_zpc_54_653_92.pdf

[57] I. Dunietz, *CP Violation with Beautiful Baryons*, Z. Phys. C **56**, 129 (1992),
http://kirkmcd.princeton.edu/examples/EP/dunietz_zpc_56_129_92.pdf

[58] B. Winstein, *CP Violation in Neutral B-Meson Decays in the Standard and Superweak Models*, Phys. Rev. Lett. **68**, 1271 (1992),
http://kirkmcd.princeton.edu/examples/EP/winstein_prl_68_1271_92.pdf

[59] R. Aleksan *et al.*, *CP Violation Using Non-CP Eigenstate Decays of Neutral B Mesons*, Nucl. Phys. **B361**, 141 (1991), http://kirkmcd.princeton.edu/examples/EP/aleksan_np_b361_141_91.pdf

[60] D. Du, I. Dunietz and D.-D. Wu, *Systematic Study of Large CP Violations in Decays of Neutral b-Flavored Mesons*, Phys. Rev. D **34**, 3414 (1986),
http://kirkmcd.princeton.edu/examples/EP/du_prd_34_3414_86.pdf

[61] I. Dunietz and J. Rosner, *Time-Dependent CP-Violation Effects in B^0-$\bar{B}^0$ Systems*, Phys. Rev. D **34**, 1404 (1986),
http://kirkmcd.princeton.edu/examples/EP/dunietz_prd_34_1404_86.pdf

[62] I.I. Bigi and A.I. Sanda, *Notes on the Observability of CP Violations in B Decays*, Nucl. Phys. **B193**, 85 (1981), http://kirkmcd.princeton.edu/examples/EP/bigi_np_b193_85_81.pdf

[63] M. Gronau and D. London, *Isospin Analysis of CP Asymmetries in B Decays*, Phys. Rev. Lett. **65**, 3381 (1990), http://kirkmcd.princeton.edu/examples/EP/gronau_prl_65_3381_90.pdf

[64] Y. Nir and H.R. Quinn, *Measuring Cabibbo-Kobayashi-Maskawa Parameters with CP Asymmetry and Isospin Analysis in $B \to \pi K$*, Phys. Rev. Lett. **67**, 541 (1991),
http://kirkmcd.princeton.edu/examples/EP/nir_prl_67_541_91.pdf

[65] H.J. Lipkin *et al.*, *Penguin Trapping with Isospin Analysis and CP Asymmetries in B Decays*, Phys. Rev. D **44**, 1454 (1991),
http://kirkmcd.princeton.edu/examples/EP/lipkin_prd_44_1454_91.pdf

[66] M. Gronau, *Elimination of Penguin Contributions to CP Asymmetries in B Decays through Isospin Analysis*, Phys. Lett. **B265**, 389 (1991),
http://kirkmcd.princeton.edu/examples/EP/gronau_pl_b265_389_91.pdf

[67] C.A. Nelson, *CP Determination and Tests for CP and P Violation by the V_1V_2 Decay Mode*, Phys. Rev. D **30**, 1937 (1984),
http://kirkmcd.princeton.edu/examples/EP/nelson_prd_30_1937_84.pdf

[68] J.R. Dell'Aquila and C.A. Nelson, *P or CP Determination by Sequential Decays: V_1V_2 Modes with Decays into $\overline{l}_A l_B$ and/or $\overline{q}_A q_B$*, Phys. Rev. D **33**, 80 (1986),
http://kirkmcd.princeton.edu/examples/EP/dellaquila_prd_33_80_86.pdf
Simple Tests for CP or P Violation by Sequential Decays: V_1V_2 Modes with Decays into $\overline{l}_A l_B$ and/or $\overline{q}_A q_B$, Phys. Rev. D **33**, 101 (1986),
http://kirkmcd.princeton.edu/examples/EP/dellaquila_prd_33_101_86.pdf

[69] G. Valencia, *Angular Correlations in the Decay $B \to VV$ and CP Violation*, Phys. Rev. D **39**, 3330 (1989),
http://kirkmcd.princeton.edu/examples/EP/valencia_prd_39_3339_89.pdf

[70] B. Kayser *et al.*, *B Hadronic Asymmetries and Spin Correlations*, Phys. Lett. **237B**,508 (1990), http://kirkmcd.princeton.edu/examples/EP/kayser_pl_237b_508_90.pdf

[71] I. Dunietz *et al.*, *How to Extract CP-Violating Asymmetries from Angular Correlations*, Phys. Rev. D **43**, 2193 (1991), http://kirkmcd.princeton.edu/examples/EP/dunietz_prd_43_2193_91.pdf

[72] G. Kramer and W.F. Palmer, *Branching Ratios and CP Asymmetries in the Decay $B \to VV$*, Phys. Rev. D **45**, 193 (1992), http://kirkmcd.princeton.edu/examples/EP/kramer_prd_45_193_92.pdf

[73] G. Kramer and W.F. Palmer, *Polarization and CP Asymmetries in the Decays $B \to K^\star\psi$, $K^\star\omega$, and $K^\star\rho$*, Phys. Lett. **B279**, 181 (1992), http://kirkmcd.princeton.edu/examples/EP/kramer_pl_b279_181_92.pdf

[74] A. Einstein, B. Podolsky and N. Rosen, *Can Quantum-Mechanical Description of Physical Reality Be Considered Complete?* Phys. Rev. **47**, 777 (1935), http://kirkmcd.princeton.edu/examples/QM/einstein_pr_47_777_35.pdf

[75] P. Oddone, Proc. UCLA Workshop on Linear Collider $B\bar{B}$ Factory Conceptual Design (1987), p. 243.

[76] D. London and R.D. Peccei, *Penguin Effects in Hadronic B Asymmetries*, Phys. Lett. **B223**, 257 (1989), http://kirkmcd.princeton.edu/examples/EP/london_pl_b223_257_89.pdf

[77] M.A. Shifman, A.I. Vainstein and V.I. Zakharov, *Asymptotic Freedom, Light Quarks and the Origin of the $\Delta T = \frac{1}{2}$ rule in the Nonleptonic Decays of Strange Particles*, Nucl. Phys. **B120**, 316 (1977), http://kirkmcd.princeton.edu/examples/EP/shifman_np_b120_316_77.pdf

[78] *The Physics Program of a High-Luminosity Asymmetric B Factory at SLAC*, SLAC-353 (Oct. 1989), http://www.slac.stanford.edu/pubs/slacreports/slac-r-353.html

[79] BCD Collaboration, *Expression of Interest for a Bottom Collider Detector at the SSC* (EOI0008), submitted to the SSC Laboratory (May 25, 1990), http://kirkmcd.princeton.edu/examples/EP/bcd_eoi.pdf

[80] C. Biino and S. Palestini, *Sensitivity to Mixing and CP Violation in the B^0-$\bar{B}^0$ Systems by Decay Distribution Study*, Riv. Nuovo Cim. **14**, 1 (1991), http://kirkmcd.princeton.edu/examples/EP/biino_rnc_14_1_91.pdf

[81] I.S. Gradshteyn and I.M. Ryzhik, *Table of Integrals, Series, and Products*, 5$^{\text{th}}$ ed. (Academic Press, 1994). http://kirkmcd.princeton.edu/examples/EM/gradshteyn_80.pdf

[82] R.A. Fisher, *On an Absolute Criterion for Fitting Frequency Curves*, Mess. Math. **41**, 155 (1912), http://kirkmcd.princeton.edu/examples/statistics/fisher_mm_41_155_12.pdf

[83] M.V. Purohit, *Measuring CP Asymmetries in B Decays* (July 14, 1992), http://kirkmcd.princeton.edu/examples/EP/purohit_071492.pdf

[84] F. Porter, *Dilution Factors in CP Violation Measurement*, BaBar Notes #24 (Jan. 25, 1990) and #26B (Feb. 9, 1990),
http://kirkmcd.princeton.edu/examples/EP/porter_babar24_012590.pdf
http://kirkmcd.princeton.edu/examples/EP/porter_babar26b_020990.pdf
The author wishes to thank Frank for a critical reading of Appendix B.